Mathematics

AIMS Mathematics, 11(2): 3563–3593.
DOI: 10.3934/math.2026146
Received: 17 November 2025
Revised: 11 January 2026
Accepted: 27 January 2026
Published: 05 February 2026

https://www.aimspress.com/journal/Math

Research article

A multivariate discrete Wiener range distribution with truncation: Theory, reliability properties, and applications to constrained financial markets

Sana Abdulkream Alharbi[1,2] and Mohamed Abd Allah El-Hadidy[3,*]

[1] Department of Mathematics and Statistics, College of Science in Yanbu, Taibah University, Yanbu Governorate, Saudi Arabia; saaharbi@taibahu.edu.sa
[2] Health and Life Research Center, Taibah University, Madinah, Saudia Arabia
[3] Mathematics Department, Faculty of Science, Tanta University, Tanta 31527, Egypt; melhadidi@science.tanta.edu.eg

* **Correspondence:** Email: melhadidi@science.tanta.edu.eg.

Abstract: We developed a multivariate discrete range distribution derived from the Wiener process to model high-low price dynamics of multiple assets observed at discrete times and subject to market imposed bounds. The model provides closed-form expressions for the joint PMF, CDF, survival and hazard functions, reversed and second order failure rates, moments, stress-strength reliability, and a full system of multivariate order statistics. A truncated version of the distribution was also established to account for realistic price limit regimes, showing how probability mass redistributes within constrained domains. These theoretical properties were supplemented by a numerical study based on real high-low data and confirmed that the model can capture clustered volatility, attenuation of tail risk, and joint range behavior more precisely than unconstrained formulations. The proposed framework offers a mathematically coherent and computationally practical tool for the analysis of range-based behavior in constrained financial markets.

Keywords: discrete range modeling; bounded price dynamics; truncated stochastic distributions; reliability measures; range-based volatility
Mathematics Subject Classification: 60E05, 60J70

1. Introduction

Using the high-low spread of a Wiener process over a specified interval provides a more informative and accurate depiction of price variability than traditional models based solely on closing prices. This modeling preference is further backed by a body of theoretical and empirical results in the finance econometrics literature. In contrast to volatility measures based on close-to-close returns, which are based on a single observation for each time interval, the price range captures the full intraperiod set of observations, leading to a superior form of efficiency in working with discrete financial data. Parkinson [1] demonstrated that the range-based estimator significantly outperforms the classical squared-return estimator under a Brownian motion framework, while Garman and Klass [2] showed that incorporating opening and closing prices further improves efficiency and reduces estimation bias. These results also indicate greater robustness of range-based estimators to microstructure noise. In parallel, the literature has proposed alternative approaches for modeling volatility and dependence in financial markets, including stochastic volatility and jump diffusion models to capture time-varying volatility and tail risk [3], copula-based multivariate frameworks for nonlinear dependence modeling [4,5], and market microstructure models incorporating price limits and circuit breakers to mitigate extreme price movements [6]. While these approaches address different aspects of market behavior, we focus on discrete range-based modeling with explicit truncation in this study, providing a coherent framework that reflects bounded price dynamics in constrained financial markets

This measure finds widespread use in short term volatility estimation, risk metric calibration, and the pricing of derivatives sensitive to extreme price changes. The pioneering work in [7], followed by subsequent contributions in [8], established a theoretical framework for the distribution of the continuous range. Further developments in [9] introduced bounded and piecewise variants that incorporate price limit mechanisms observed in real financial markets. These results together support the price range as a strong and reliable instrument for financial data modeling, particularly when the dynamics of asset prices occur over bounded intervals.

In addition to its theoretical advantages and empirical support, the price range has proven to be highly relevant in practical financial applications. Building on the documented empirical efficiency and robustness of range-based volatility measures in discretely observed financial data, the following analysis focuses on modeling the price range within a discrete and constrained probabilistic framework. Actual financial data are often measured at discrete points in time, such as days or months, which calls for the use of discrete distributions rather than continuous ones. Discrete versions of several well known distributions, such as the normal distribution as in [10,11] and the Weibull distribution as in [12,13], have been developed to suit the nature of discrete data. Based on this, El-Hadidy [14] proposed a discrete distribution of the range of the Wiener process by a number dependent transformation and demonstrated that it has very good agreement with real financial data. El-Hadidy and Alfreedi [15] introduced a new model for a Wiener process range distribution by the application of internal truncation, with a view to remove low stochastic volatility intervals and redistributing their probability to the active intervals. Their results showed that the modified distribution captures price moves more effectively in volatile markets and is, hence, appropriate for use in financial modeling.

On the other hand, most previous studies have been confined to univariate models, whereas modern financial markets increasingly rely on multivariate frameworks to characterize dependence and correlation among multiple assets. Accordingly, multivariate distributions play a central role in risk management and portfolio analysis, including the multivariate normal distribution and

copula-based models, as discussed in [4,5,16]. These researchers have proposed several alternative approaches for modeling multivariate dependence in financial markets. Copula-based models construct dependence by first specifying marginal distributions and then imposing a dependence structure through a copula function, thereby enabling flexible nonlinear and tail dependence. Other approaches include multivariate stochastic volatility and jump diffusion models, which introduce latent volatility dynamics and discontinuities to capture time varying risk and extreme events [3]. In a related line of research, Alraddadi and El-Hadidy [17] developed a multivariate distribution of the continuous Wiener process range using probability range vectors, enabling the characterization of complex temporal relationships among asset price behaviors. In contrast to these approaches, the model proposed in this study differs conceptually in that dependence arises directly from the joint distribution of the discrete price ranges, within a unified, discrete, and truncated framework that provides a structurally coherent representation of joint range behavior under regulatory constraints, rather than imposing dependence ex post as in copula-based formulations.

However, discretizing the range of a Wiener process poses substantially greater technical challenges than discretizing its levels or increments. While levels and increments are local quantities defined at fixed time points or over disjoint intervals and benefiting from the independence and stationarity of Brownian increments, the range is a global, path-dependent functional defined through the joint behavior of the supremum and infimum of the process over a time interval. As a result, the range inherently couples two extreme values and exhibits strong nonlinear dependence that cannot be captured through standard discretization schemes applied to levels or increments. In particular, naïve discretization may distort tail probabilities or violate probabilistic normalization. In the univariate case, this difficulty was addressed in [14] by discretizing the survival function of the continuous Wiener range and defining the discrete probability mass function via successive differences. Extending this construction to the multivariate setting, as carried out in this present work, is nontrivial since it requires preserving the global extreme value structure of each marginal range while ensuring joint consistency, proper normalization over a multidimensional lattice, and analytical tractability for multivariate reliability measures and truncation under market-imposed bounds

In recent studies, researchers have examined truncated Wiener process models, particularly in reliability and risk analysis under bounded conditions. In the continuous framework, Pan et al. [18] developed reliability models based on truncated Wiener processes using truncated normal distributions, which are conceptually related to this work but differ from thier discrete formulation. Related contributions include [19] on truncated distributions and information measures, and [20] on multivariate models for finance and reliability. Moreover, Alraddadi and El-Hadidy [17] proposed a continuous multivariate Wiener range model under stochastic volatility and truncation. In contrast, we introduce a fully discrete, multivariate Wiener range distribution with explicit truncation and closed-form reliability measures, tailored to discretely observed and constrained financial data. The Wiener process assumption is adopted here as a standard modeling approximation, without formal empirical validation.

The originality and scientific contribution of this work lie in the distinction it offers from other studies by introducing a new statistical framework that combines discreteness, multiplicity, and truncation, making it more suitable for the nature of financial data observed at discrete intervals and subject to daily price constraints. While in previous literature, researchers have focused on the range distributions of the Wiener process in continuous or single period versions, the current model fills an important research gap by directly representing regulatory constraints and deriving risk indicators (such as survival and hazard functions and rank statistics). Real world data is employed to demonstrate that the proposed model effectively reflects the dynamics of constrained markets,

enhancing its potential for use in pricing and risk management, outperforming classical continuous or single period models. Accordingly, we aim to develop and present a multivariate, independent, discrete distribution of the Wiener process range, where each variable is used to represent the difference between the highest and lowest prices of an independent stock over discrete time periods. This includes deriving the bivariate case of this distribution and its truncated version under stochastic volatility to analyze the joint interaction between the ranges of two independent stocks and its impact on the accuracy of financial modeling. Additionally, we study the basic statistical properties of this distribution, including reliability functions, moments, stress-strength parameter, and ordered statistics. The proposed framework yields closed-form expressions for the joint probability mass function, survival and hazard functions (with monotonicity properties), and a complete system of multivariate order statistics, thereby highlighting the analytical depth of the model.

The paper is organized as follows: In Section 2, we study the discrete multivariate distribution of the n independent Wiener processes range, which captures the difference between the highest and lowest stock prices over fixed time intervals. In Section 3, we discuss the bivariate case of this distribution, its truncated version, and some basic distributional properties. In Section 4, a detailed numerical application is carried out using randomly generated data that simulates the behavior of real life restricted markets. This application includes statistical analysis and simulation of the joint movement of the price range under truncated distribution conditions, with the aim of verifying the practical suitability of the proposed model. Concluding remarks and future recommendations are discussed in Section 5.

2. *n*-multivariate discrete distribution for a Wiener process range

Definition 1. If the range of a Wiener process $\{W(t); t \geq 0\}$ is defined as

$$R(T) = \underset{(0,T)}{sup} W(t) - \underset{(0,T)}{inf} W(t),$$

(a difference between the maximum and minimum values of a Brownian path measured at a finite number of discrete points in time), and if n points are assumed in the interval $(0,T)$, then a discrete distribution of $R(T)$ is obtained by applying a number dependent transformation, via discretization of the survival function, of the corresponding continuous range distribution. Specifically, the probability mass function (PMF) of the discrete Wiener range is defined as,

$$\begin{aligned}\widetilde{f}_{R(T)}(r) &= P[R(T) = r] = P[R(T) \geq r] - P[R(T) \geq r+1] \\ &= \sum_{k=1}^{\infty} \left[\left(C_k + 8T(r+1)^{-2}\right) \exp\left[-4TC_k^{-1}(r+1)^{-2}\right] - \left(C_k + 8Tr^{-2}\right) \exp\left[-4TC_k^{-1}r^{-2}\right] \right], \end{aligned} \tag{2.1}$$

where

$$r = 0,1,2,\ldots,\ 0 < r < \infty,\ T > 0, C_k = \frac{8}{(2k-1)^2\pi^2}$$

and the survival function $P[R(T) \geq r]$ is derived from the continuous distribution of the Wiener process range. This construction guarantees a valid discrete PMF while preserving the extreme-value nature of the continuous range distribution [7,8].

Function (2.1) is derived using a method based on the maximum and minimum distribution of the process, and then mathematically integrated to obtain an accurate range distribution, as in [14]. In practical financial applications, asset prices are recorded at discrete time points rather than

continuously. Accordingly, the continuous range $R(T)$ is discretized by assuming that the Wiener process is observed at a finite number of discrete intervals within $(0,T)$. The difference between the high and low values at these discrete observations creates valued variable that captures the high-low range of the process. Therefore, the continuous range distribution is estimated by discrete increments, and the probability of every value of the potential range is determined as

$$P[R(T)=r]=P[R(T)\geq r]-P[R(T)\geq r+1].$$

This change preserves the Wiener process's stochastic nature while enabling the model to be sensitive to the empirical nature of financial data over discrete (say, daily or hourly) intervals. It is evident that:

$$\sum_{r=0}^{\infty}P[R(T)=r]=P[R(T)\geq 0]-P[R(T)\geq 1]+P[R(T)\geq 1]-P[R(T)\geq 2]+\ldots=P[R(T)\geq 0]=S_{R(T)}(0)=1,$$

where $S_{R(T)}(.)$ is the survival function of $R(T)$. Accordingly, we formulate a multivariate discrete distribution representing the differences between the maximum and minimum prices (ranges) of n independent stocks, each modeled by a discrete range of an independent Wiener process over the time interval $(0,T)$, as given by:

$$\left[R_1(T),R_2(T),\ldots,R_n(T)\right]=\left[\sup_{(0,T)}W_1(t)-\inf_{(0,T)}W_1(t),\sup_{(0,T)}W_2(t)-\inf_{(0,T)}W_2(t),\ldots,\sup_{(0,T)}W_n(t)-\inf_{(0,T)}W_n(t)\right],$$

where $\left[W_1(t),W_2(t),\ldots,W_n(t)\right]$ is a vector of n independent Wiener process.

Theorem 1. Let $\boldsymbol{R(T)}=[R_1(T),R_2(T),\ldots,R_n(T)]$ be a vector of discrete ranges of $\left[W_1(t),W_2(t),\ldots,W_n(t)\right]$ over the interval $(0,T)$, where the marginal PMF of $R_i(T)$ is defined as in Definition 1, then the joint PMF of the multivariate discrete Wiener range vector $\boldsymbol{R(T)}$ is,

$$f_{R_1(T),R_2(T),\ldots,R_n(T)}(r_1,r_2,\ldots,r_n;T)=\prod_{i=1}^{n}f_{R_i(T)}(r_i). \tag{2.2}$$

Moreover, the joint distribution is properly normalized, that is,

$$\sum_{r_1=0}^{\infty}\cdots\sum_{r_n=0}^{\infty}f_{R_1(T),R_2(T),\ldots,R_n(T)}(r_1,r_2,\ldots,r_n;T)=\prod_{i=1}^{n}\left(\sum_{r_i=0}^{n}f_{R_i(T)}(r_i)\right)=1.$$

Proof. The result follows from the fact that each univariate marginal PMF $\widetilde{f}_{R_i(T)}(r)$ is a properly defined discrete probability distribution with total mass one, and independence implies that the joint PMF is the product of the marginal's. Thus, this completes the proof, where

$$\sum_{r_1=0}^{\infty}\cdots\sum_{r_n=0}^{\infty}f_{R_1(T),R_2(T),\ldots,R_n(T)}(r_1,r_2,\ldots,r_n;T)=\prod_{i=1}^{n}\left(\sum_{r_i=0}^{n}f_{R_i(T)}(r_i)\right)=1.$$

In addition, to avoid ambiguity in the discrete formulation, the joint cumulative distribution function (CDF) is derived explicitly as follows: By independence of the components $R_i(T)$, $i=1,2,\ldots,n$, we have,

$$F_{R_1(T),R_2(T),\ldots,R_n(T)}(r_1,r_2,\ldots,r_n;T)=\prod_{i=1}^{n}P[R_i(T)\leq r_i].$$

Since the range is a discrete nonnegative random variable, each marginal CDF satisfies

$$P[R_i(T) \le r_i] = 1 - P[R_i(T) \ge r_i] + P[R_i(T) = r_i]$$

which makes the discrete shift $r_i + 1$ explicit. Therefore, the joint CDF can be written as

$$F_{R_1(T),R_2(T),\ldots,R_n(T)}(r_1, r_2, \ldots, r_n; T) = \prod_{i=}^{n} (1 - P[R_i(T) \ge r_i + 1])$$
$$= \prod_{i=1}^{n} \sum_{k=1}^{\infty} [(C_k + 8T(r_i + 1)^{-2})\, exp[-4TC_k^{-1}(r_i + 1)^{-2}]]. \quad (2.3)$$

Since the sequence $\{C_k\}_{k\ge1}$ is defined in Definition 1 and satisfies $\sum_{k=1}^{\infty} C_k = 1$, then

$$F_{R_1(T),R_2(T),\ldots,R_n(T)}(\infty, \infty, \ldots, \infty; T) = 1.$$

This will also give the joint survival function by,

$$S_{R_1(T),R_2(T),\ldots,R_n(T)}(r_1, r_2, \ldots, r_n; T) = 1 - F_{R_1(T),R_2(T),\ldots,R_n(T)}(r_1, r_2, \ldots, r_n; T)$$
$$= 1 - \prod_{i=1}^{n} \sum_{k=1}^{\infty} [(C_k + 8T(r_i + 1)^{-2})\, exp[-4TC_k^{-1}(r_i + 1)^{-2}]]. \quad (2.4)$$

3. Discrete bivariate distribution and its truncated version

When analyzing high frequency financial data, the discrete binomial distribution is an effective tool for modeling the interdependence of stock price changes at discrete points in time. Koopman et al. [21] presented an advanced model based on the distribution of Skellam [22] that uses a discrete copula function to represent price differences. This distribution gives the difference between two independent random variables that follow a Poisson distribution. This distribution is a natural extension of continuous distributions such as the Wiener process to the discrete case, as the discrete distribution enables an accurate representation of minute price changes in financial markets. These distributions contribute to the fair pricing of digital options, joint risk assessment, and understanding the temporal structure of price correlation between stocks, which increases the efficiency of trading and forecasting strategies, as in [23]. Therefore, from (2.2), the joint PMF of a Wiener range random variables $R_1(T)$ and $R_2(T)$ is,

$$f_{R_1(T),R_2(T)}(r_1, r_2; T) = \prod_{i=1}^{2} \sum_{k=1}^{\infty} \left[\left(C_k + 8T(r_i+1)^{-2}\right) \exp\left[-4TC_k^{-1}(r_i+1)^{-2}\right] - \left(C_k + 8Tr_i^{-2}\right) \exp\left[-4TC_k^{-1} r_i^{-2}\right] \right], \quad (3.1)$$

$0 \le r_i \le \infty, i = 1, 2$, as shown in Figure 1.

Remark 1. All figures presented in this paper (Figures 1–12) follow a unified visualization scheme in which the continuous Wiener range distribution is displayed side by side with its discrete counterpart (and truncated versions where applicable). This parallel presentation provides a clear conceptual comparison between the theoretical continuous formulation and the discrete model developed in this study, clarifies the transition from the continuous to the discrete framework, and highlights the theoretical coherence of the proposed discrete multivariate Wiener range distribution.

For all numerical figures presented in this paper, the time horizon is fixed at $T = 1$. The truncation bounds are kept unchanged across all simulations and are directly indicated by the visible support of the plotted distributions in the figures. Figure 1(a) represents the joint probability density function of the two random variables $R_1(T)$ and $R_2(T)$ in the continuous case, where the distribution

is accurately represented in two-dimensional space. Figure 1(b) represents the joint PMF of the same variables after discretization (i.e., converting continuous random variables to discrete ones). Thus, Figure 1(a) is a numerical approximation of Figure 1(b), demonstrating how the theoretical continuous distribution can be represented in a form that is applicable numerically or programmatically.

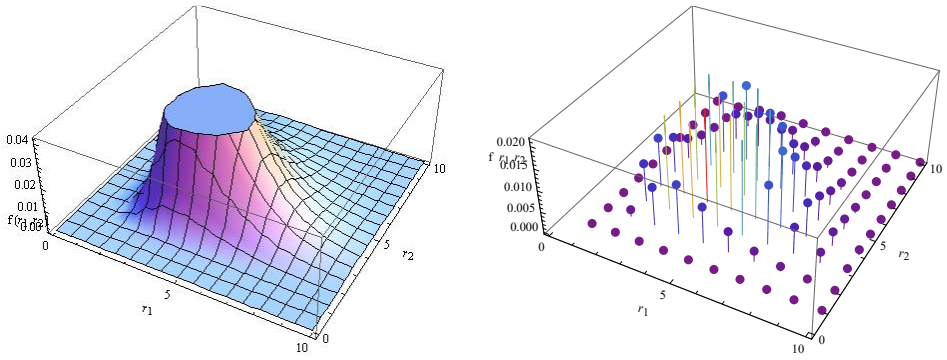

(a) **(b)**

Figure 1. The joint bivariate probability function in **(a)** continuous case; and **(b)** discrete case.

On the other hand, the truncated joint probability density function of $R_1(T)$ and $R_2(T)$ on the interval $[a_i, b_i], i = 1,2$ is given by,

$$\bar{f}_{\bar{R}_i(T),\bar{R}_2(T)}(\bar{r}_1, \bar{r}_2; T) = \prod_{i=1}^{2} \frac{f_{\bar{R}_i(T)}(\bar{r}_i)}{F_{R_i(T)}(b_i) - F_{R_i(T)}(a_i)},\ a_i \le \bar{r}_i \le b_i, i = 1,2$$

$$= \prod_{i=1}^{2} \frac{\sum_{k=1}^{\infty}\left[\left(C_k + 8T(\bar{r}_i+1)^{-2}\right)\exp\left[-4C_k^{-1}T(\bar{r}_i+1)^{-2}\right] - \left(C_k + 8T\bar{r}_i^{-2}\right)\exp\left[-4C_k^{-1}T\bar{r}_i^{-2}\right]\right]}{\sum_{k=1}^{\infty}\left[\left(C_k + 8T(b_i+1)^{-2}\right)\exp\left[-4C_k^{-1}T(b_i+1)^{-2}\right]\right] - \sum_{k=1}^{\infty}\left[\left(C_k + 8T(a_i+1)^{-2}\right)\exp\left[-4C_k^{-1}T(a_i+1)^{-2}\right]\right]}, \quad (3.2)$$

where $\bar{R}_i(T)$ is a corresponding double truncated (truncation from left and right) of $R(T)$ and $r_i = a_i, \ldots, a_i + \tilde{i}, \ldots, b_i$, and $\tilde{i}$ is a non negative real number. In this case, the probabilistic support is restricted to a known range that reflects constraints imposed on variables, such as the high and low price limits of stocks. In this context, using a truncated version of this distribution enables modeling price differences within a precisely defined range, while preserving the basic properties of the original distribution. This distribution is essential in high-frequency applications, where data are effectively restricted to narrow ranges due to market regulations or institutional constraints. Truncated versions are also used to estimate the probability of exceeding critical limits, which increases the accuracy of forecasts of price spikes and stop-out probabilities in instruments such as binary or marginal options. Figure 2 illustrates how the continuous distribution function transforms into a discrete form through numerical approximation. Figure 2(a) represents the joint truncated probability density function in the continuous case, while Figure 2(b) shows the corresponding discrete form.

In cases where stock price differences are treated over small time intervals, the discrete bivariate distribution of quantiles is used to represent the joint cumulative distribution function at specific points in time. This discrete version of the cumulative distribution function enhances the reliability of

time correlation analyses, pricing derivatives across multiple assets, and guiding optimal diversification policies in investment portfolios. From (2.3), the joint CDF of $R_1(T)$ and $R_2(T)$ is given by,

$$F_{R_1(T),R_2(T)}(r_1,r_2;T)=\prod_{i=1}^{2}\sum_{k=1}^{\infty}\left[\left(C_k+8T(r_i+1)^{-2}\right)\exp\left[-4TC_k^{-1}(r_i+1)^{-2}\right]\right],\ 0\le r_i\le\infty, i=1,2\,. \tag{3.3}$$

see Figure 3, where Figure (3c) shows the joint CDF of a continuous bivariate distribution, where the cumulative probability values are smoothly projected into 2-dimensional space. After applying a discretization process to the random variables, this distribution is transformed into a discrete representation as in Figure (3d), where the function takes values on a grid of discrete points. This transformation demonstrates how a theoretical continuous distribution can be approximated to a numerical form suitable for computation, without losing the overall structure of the cumulative function, enabling it to be used in quantitative modeling of risk and co-dependency in a practical way.

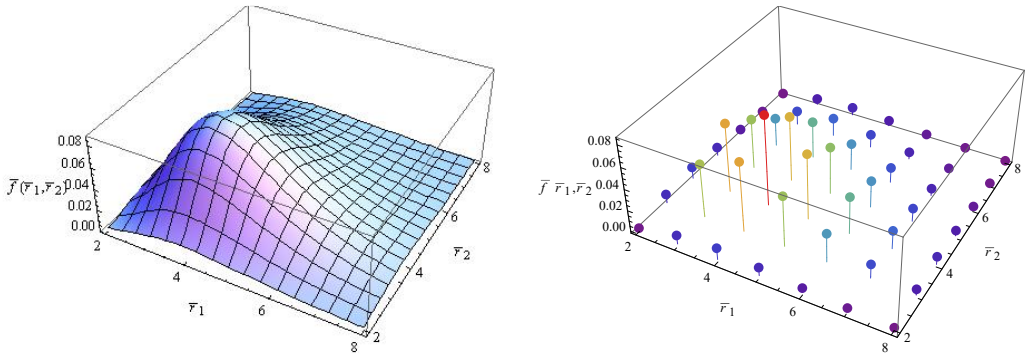

(a) **(b)**

Figure 2. The joint bivariate truncated probability function in (a) continuous case; and (b) discrete case.

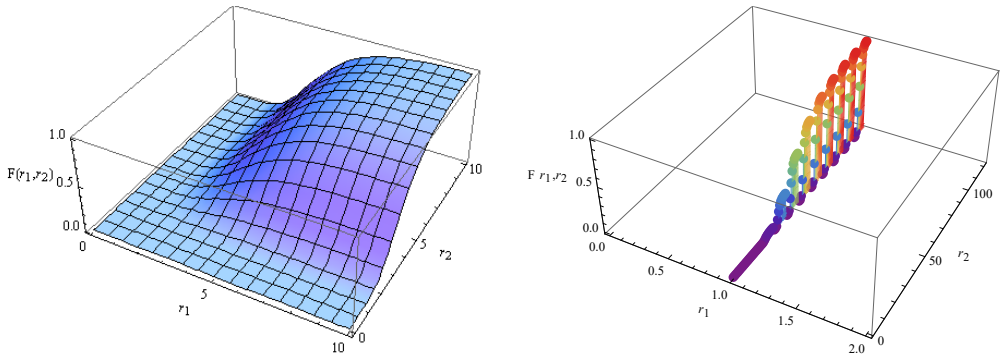

(a) **(b)**

Figure 3. The joint bivariate CDF **(a)** continuous case; and **(b)** discrete case.

The truncated CDF of the discrete bivariate distribution is used to represent the joint probabilities of stock price fluctuations within a specified price range, such as in markets that impose upper and lower limits on daily movement. This representation enables an accurate description of the

dependence between assets when random variables are confined to a grid of discrete values within a closed domain. From a market microstructure perspective, the truncation considered in this bivariate model is directly motivated by regulatory mechanisms such as daily price limits and circuit breakers, which impose explicit bounds on price movements and may interrupt trading during extreme volatility episodes. Such institutional features are widely documented in financial markets and have been shown to affect price dynamics and volatility behavior [6, 24]. Hence, from (3.2) and for a bounded range $a_i < \bar{r}_i < b_i, i = 1,2$, the joint double truncated CDF is given by,

$$\overline{F}_{\overline{R}_1(T),\overline{R}_2(T)}(\bar{r}_1,\bar{r}_2;T)=\prod_{i=1}^{2}\frac{\sum_{k=1}^{\infty}\left[\left(C_k+8T(\bar{r}_i+1)^{-2}\right)\exp\left[-4C_k^{-1}T(\bar{r}_i+1)^{-2}\right]-\left(C_k+8T(a_i+1)^{-2}\right)\exp\left[-4C_k^{-1}T(a_i+1)^{-2}\right]\right]}{\sum_{k=1}^{\infty}\left[\left(C_k+8T(b_i+1)^{-2}\right)\exp\left[-4C_k^{-1}T(b_i+1)^{-2}\right]-\left(C_k+8T(a_i+1)^{-2}\right)\exp\left[-4C_k^{-1}T(a_i+1)^{-2}\right]\right]}, \quad (3.4)$$

(see Figure 4). The joint truncated CDF of bivariate distribution over a specified range is reflected in Figure (4c). Figure (4d) shows its counterpart after numerical approximation to a discrete distribution. This demonstrates how the cumulative structure does not change even as it is confined to fit into a numerical expression to facilitate its effective use in bound constraint models by price ceilings.

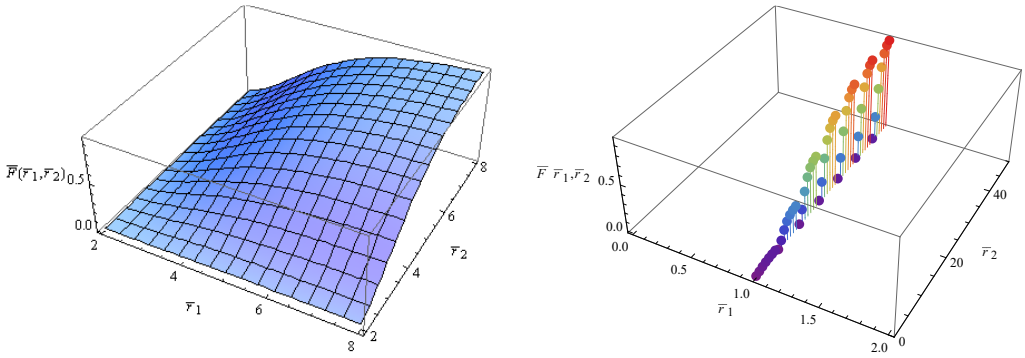

(a) **(b)**

Figure 4. The joint bivariate truncated CDF **(a)** continuous case; and **(b)** discrete case.

The joint survival function of a discrete bivariate distribution is used to estimate the probability of stock price fluctuations exceeding certain thresholds, making it a powerful tool in extreme risk analysis. Using (3.3), we can compute it by,

$$S_{R_1(T),R_2(T)}(r_1,r_2;T)=1-F_{R_1(T),R_2(T)}(r_1,r_2;T).$$

When the domain is restricted by truncated support, the function becomes even more important because it represents the remaining probabilities within a realistic range that reflects the limits of price movement. Additionally, one can compute the truncated case of this function from (3.4) by,

$$\bar{S}_{\bar{R}_1(T),\bar{R}_2(T)}(\bar{r}_1,\bar{r}_2;T)=1-\bar{F}_{\bar{R}_i(T),\bar{R}_2(T)}(\bar{r}_1,\bar{r}_2;T).$$

Figures 5 and 6, which contain Figures 5(c,d) and 6(c,d), reflect the transformation from the joint survival function of the continuous bivariate distribution to its discrete counterpart, while keeping the probability structure in the right tail within a specified range. The discrete survival function enables the characterization of tail dependence and is used in practical applications in marginal option valuation models and in detecting co-excesses in multi-asset portfolios.

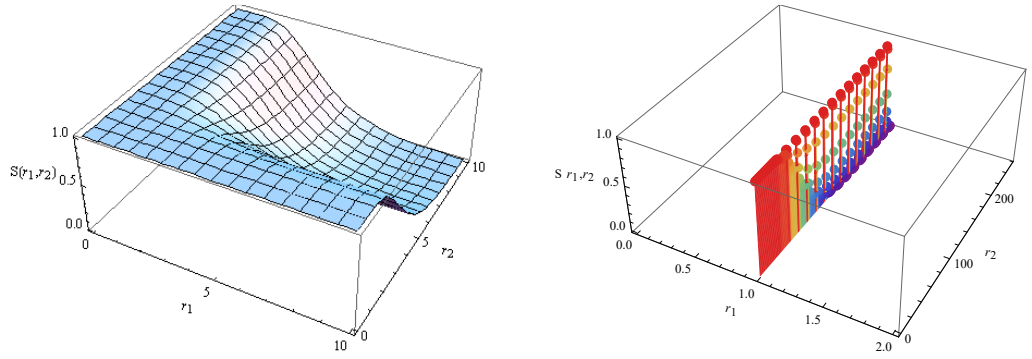

(a) **(b)**

Figure 5. The joint bivariate survival function **(a)** continuous case; and **(b)** discrete case.

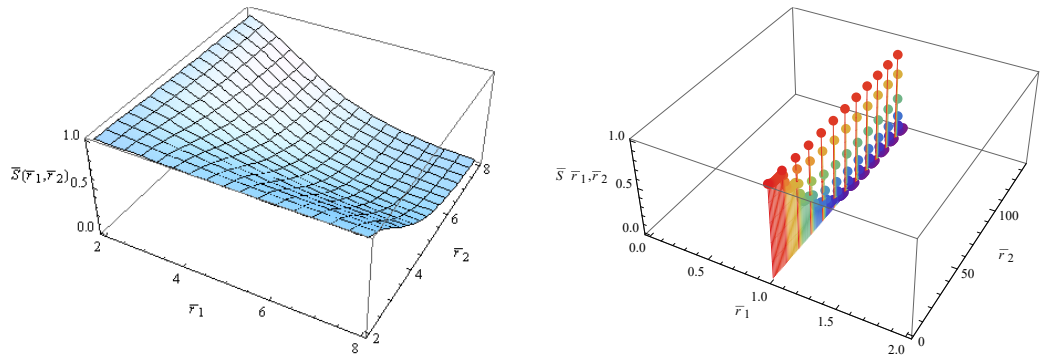

(a) **(b)**

Figure 6. The joint bivariate truncated survival function **(a)** continuous case; and **(b)** discrete case.

3.1. *Some reliability properties*

Given the need to measure stock price behavior over specific time periods (daily, monthly, or annually), studying the basic distributional properties of this distribution as a discrete distribution is crucial. This includes analyzing the reliability properties, which measure the stability of the price range, as well as the moments used to calculate the mean and variance, which describe the centralization and dispersion characteristics of price differences. The stress-strength parameter is also used to estimate the probability of one price change being larger than another. Bonferroni and Lorenz curves are useful for summarizing the variance of a distribution, and the Gini index provides a quantitative estimate of the asymmetrical distribution of returns. Together, these indices enable us to estimate the probability structure and variance of price changes in a realistic discrete probability model.

Reliability theory provides a natural and powerful framework for analyzing range-based financial risk, as it focuses on time-to-event behavior and conditional risk evolution rather than marginal price changes. When applied to the high-low price range, reliability measures such as the hazard rate, reversed hazard rate, and mean residual life offer interpretable indicators of the likelihood, timing, and persistence of extreme price movements within bounded markets. This perspective is particularly suitable for range-based modeling, where risk accumulation is inherently linked to the widening of price spreads under regulatory or structural constraints. In economic risk analysis, the discrete multivariate hazard ratio is used as a tool to measure the probability of a sudden change in stock prices

over discrete time periods. This indicator expresses the probability of a price change in a financial asset, provided the price has remained within specified upper and lower bounds up to that point, making it suitable for price-constrained market models. When applied to distributions such as the discrete bivariate distribution of the Wiener process range, the hazard ratio can reflect the interdependence of different assets and the timing of risk occurrences, making it of practical importance in the fields of reliability theory, time-risk estimation, and modeling extreme changes in multi-asset portfolios.

In price constrained market models, the discrete multivariate distribution hazard function is a powerful tool for analyzing the intertemporal risks associated with asset price changes. Using the discrete Wiener process range distribution, the probability of sharp price changes at a given point in time can be estimated, given that the price range remains within a specified range up to that point. Marshall and Olkin [25] have pointed out the importance of hazard functions in characterizing the behavior of breakdowns or structural transformations in economic systems. Therefore, using the hazard function within this framework enhances the accuracy of extreme risk estimation and contributes to the design of derivative instruments based on the conditional probability of price overshoot in regulated markets.

Proposition 1. If $R_1(T)$ and $R_2(T)$ are two independent discrete range variables of Wiener processes over the interval $(0,T)$, then the joint discrete hazard rate function of the bivariate range vector $[R_1(T), R_2(T)]$ is defined by,

$$H_{R_1(T),R_2(T)}(r_1,r_2;T) = P(R_1(T)=r_1, R_2(T)=r_2 | R_1(T)\geq r_1, R_2(T)\geq r_2),\ r_1,r_2 = 0,1,2,\ldots$$

$$= \prod_{i=1}^{2}\left[\frac{\sum_{k=1}^{\infty}[(C_k+8T(r_i+1)^{-2})\,exp[-4TC_k^{-1}(r_i+1)^{-2}]-(C_k+8Tr_i^{-2})\,exp[-4TC_k^{-1}r_i^{-2}]]}{1-\sum_{k=1}^{\infty}[(C_k+8T(r_i+1)^{-2})\,exp[-4TC_k^{-1}(r_i+1)^{-2}]]}\right]. \tag{3.5}$$

Proof. By definition, the joint discrete hazard rate of the bivariate range vector $[R_1(T), R_2(T)]$ is given by the conditional probability, $P(R_1(T)=r_1, R_2(T)=r_2 | R_1(T)\geq r_1, R_2(T)\geq r_2)$. Using the definition of conditional probability and since $P[R_i(T)\geq r_i]>0$, then, as in [26], the joint discrete hazard rate function can be written as,

$$H_{R_1(T),R_2(T)}(r_1,r_2;T) = \prod_{i=1}^{2}\frac{P[R_i(T)=r_i]}{P[R_i(T)\geq r_i]},$$

Since $R_1(T)$ and $R_2(T)$ are assumed to be independent random variables, the joint probability in the numerator factorizes into the product of the marginal probability mass functions, and the joint survival probability in the denominator factorizes into the product of the marginal survival functions. Hence,

$$H_{R_1(T),R_2(T)}(r_1,r_2;T) = \frac{f_{R_1(T)}(r_1;T).f_{R_2(T)}(r_2;T)}{P[R_1(T)\geq r_1].P[R_2(T)\geq r_2]}$$

$$= \prod_{i=1}^{2}\left[\frac{\sum_{k=1}^{\infty}[(C_k+8T(r_i+1)^{-2})\,exp[-4TC_k^{-1}(r_i+1)^{-2}]-(C_k+8Tr_i^{-2})\,exp[-4TC_k^{-1}r_i^{-2}]]}{1-\sum_{k=1}^{\infty}[(C_k+8T(r_i+1)^{-2})\,exp[-4TC_k^{-1}(r_i+1)^{-2}]]}\right],$$

which is non-decreasing in both r_1 and r_2 under the assumption that the marginal range distributions satisfy an increasing failure rate (IFR) property, i.e., for fixed T,

$$H_{R_1(T),R_2(T)}(r_1+1,r_2;T) \geq H_{R_1(T),R_2(T)}(r_1,r_2;T)$$

and

$$H_{R_1(T),R_2(T)}(r_1, r_2 + 1; T) \geq H_{R_1(T),R_2(T)}(r_1, r_2; T) .$$

This reflects the intuitive financial insight that, as the observed high-low range increases, the risk (or hazard) of observing that exact range also increases relative to the remaining tail probability. This formulation and its monotonicity properties are consistent with standard results in discrete reliability and multivariate hazard theory [25,27,28].

The hazard rate function is utilized in the censored discrete multivariate distribution for probability estimation of price movement in a specified range with an upper and lower bound. The depiction provides a realistic representation of the dynamics of price-constrained markets and the timing of cross-asset risk. For our distribution, the joint truncated hazard rate function in the bivariate case is given by,

$$\overline{H}_{\overline{R}_1(T),\overline{R}_2(T)}(\bar{r}_1,\bar{r}_2;T) = \bar{f}_{\overline{R}_1(T),\overline{R}_2(T)}(\bar{r}_1,\bar{r}_2;T)\{1-\overline{F}_{\overline{R}_1(T),\overline{R}_2(T)}(\bar{r}_1,\bar{r}_2;T)\}^{-1}$$

$$= \prod_{i=1}^{2}\left[\frac{\sum_{k=1}^{\infty}\left[\left(C_k+8T(r_i+1)^{-2}\right)\exp\left[-4TC_k^{-1}(r_i+1)^{-2}\right]-\left(C_k+8Tr_i^{-2}\right)\exp\left[-4TC_k^{-1}r_i^{-2}\right]\right]}{\sum_{k=1}^{\infty}\left[\left(C_k+8T(b_i+1)^{-2}\right)\exp\left[-4TC_k^{-1}(b_i+1)^{-2}\right]-\sum_{k=1}^{\infty}\left[\left(C_k+8T(a_i+1)^{-2}\right)\exp\left[-4TC_k^{-1}(a_i+1)^{-2}\right]\right]}{1-\frac{\sum_{k=1}^{\infty}\left[\left(C_k+8T(r_i+1)^{-2}\right)\exp\left[-4TC_k^{-1}(r_i+1)^{-2}\right]-\left(C_k+8T(a_i+1)^{-2}\right)\exp\left[-4TC_k^{-1}(a_i+1)^{-2}\right]\right]}{\sum_{k=1}^{\infty}\left[\left(C_k+8T(b_i+1)^{-2}\right)\exp\left[-4TC_k^{-1}(b_i+1)^{-2}\right]-\left(C_k+8T(a_i+1)^{-2}\right)\exp\left[-4TC_k^{-1}(a_i+1)^{-2}\right]\right]}}\right]. \quad (3.6)$$

It should be noted that the truncated hazard function in (3.6) is defined with respect to the truncated joint distribution and follows the standard discrete hazard formulation

$$\frac{\bar{f}_{\bar{R}_1(T),\bar{R}_2(T)}(\bar{r}_1,\bar{r}_2;T)}{1-\bar{F}_{\bar{R}_1(T),\bar{R}_2(T)}(\bar{r}_1,\bar{r}_2;T)}.$$

This definition represents a different multivariate hazard construction from the product of marginals formulation in Proposition 1 and is commonly adopted in the reliability literature when truncation or conditioning is involved [25,27,28].

Figures 7 and 8 illustrate the shift from the continuous to the discrete joint hazard rate functions for the original and truncated distributions, respectively.

Additionally, at $r_1 = r_2 = 0$, one can notice that,

$$H_{R_1(T),R_2(T)}(0,0;T) = f_{R_1(T),R_2(T)}(0,0;T) = (\textstyle\sum_{k=1}^{\infty}(C_k + 8T)\, exp[-4C_k^{-1}T])^2, \quad (3.7)$$

and

$$\overline{H}_{\overline{R}_1(T),\overline{R}_2(T)}(0,0;T) = \bar{f}_{\overline{R}_1(T),\overline{R}_2(T)}(0,0;T)$$

$$= \left(\frac{\sum_{k=1}^{\infty}\left[\left(C_k+8T\right)\exp\left[-4C_k^{-1}T\right]\right]}{\sum_{k=1}^{\infty}\left[\left(C_k+8T(b_i+1)^{-2}\right)\exp\left[-4C_k^{-1}T(b_i+1)^{-2}\right]-\sum_{k=1}^{\infty}\left[\left(C_k+8T(a_i+1)^{-2}\right)\exp\left[-4C_k^{-1}T(a_i+1)^{-2}\right]\right]}\right)^2. \quad (3.8)$$

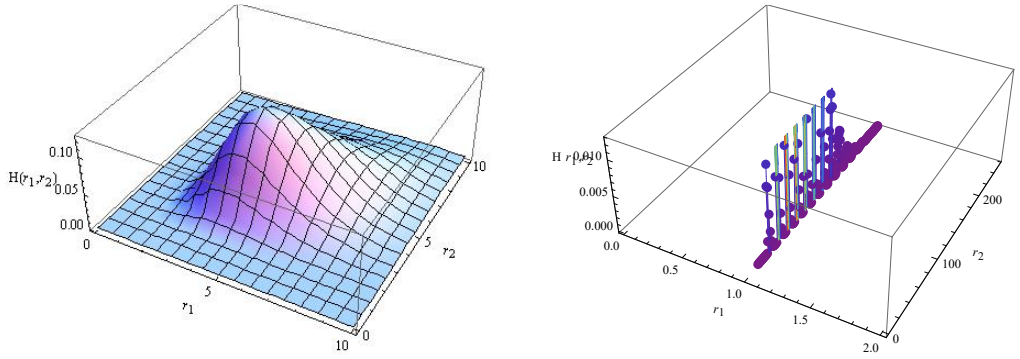

(a) **(b)**

Figure 7. The joint bivariate hazard rate function **(a)** continuous case; and **(b)** discrete case.

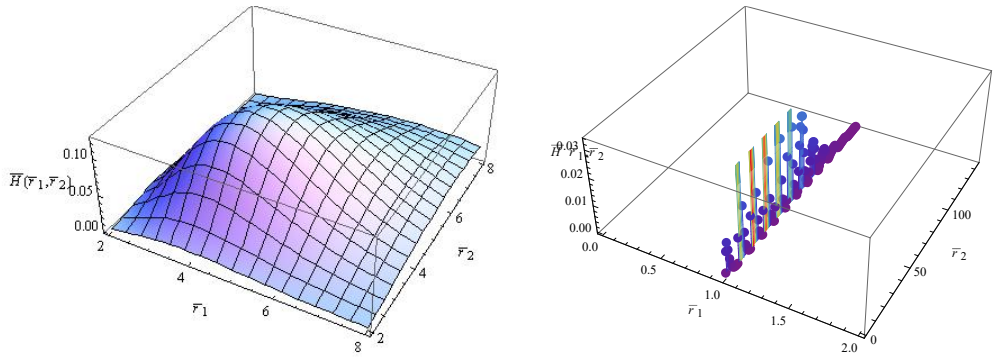

(a) **(b)**

Figure 8. The joint bivariate truncated hazard rate function **(a)** continuous case; and **(b)** discrete case.

Corollary 1. For the original bivariate case, the joint mean residual life function is given by,

$$L_{R_1(T),R_2(T)}(r_1,r_2;T)=\prod_{i=1}^{2}E\left[(R_i(T)-r_i)\middle|R_i(T)\geq r_i\right]=\prod_{i=1}^{2}\left(\frac{\sum_{j\geq r_i}jf_{R_i(T)}(j)}{\sum_{j\geq r_i}f_{R_i(T)}(j)}-r_i\right) \tag{3.9}$$

$$=\prod_{i=1}^{2}\left(\frac{\sum_{j\geq r_i}S_{R_i(T)}(j)}{S_{R_i(T)}(r_i)}\right)=\prod_{i=1}^{2}\sum_{j\geq r_i}\prod_{i=r_i}^{j}(1-H_{R_i(T)}(i))$$

$$=\prod_{i=1}^{2}\left(\sum_{j\geq r_i}\prod_{i=r_i}^{j}\left[\frac{1+\sum_{k=1}^{\infty}\left[\left(C_k+8Ti^{-2}\right)\exp\left[-4C_k^{-1}Ti^{-2}\right]-2\left(C_k+8T(i+1)^{-2}\right)\exp\left[-4C_k^{-1}T(i+1)^{-2}\right]\right]}{1-\sum_{k=1}^{\infty}\left[\left(C_k+8T(i+1)^{-2}\right)\exp\left[-4C_k^{-1}T(i+1)^{-2}\right]\right]}\right]\right),$$

where $r=0,1,2,\ldots$.

Corollary 2. As in Roy and Gupta [29], another formula for this function is given by,

$$\mu_{R_1(T),R_2(T)}(r_1,r_2;T)=\prod_{i=1}^{2}\left(E\left[(R_i(T)-r_i)\middle|R_i(T)\geq r_i\right]\right)=1+\prod_{i=1}^{2}L_{R_i(T)}(r_i+1)$$

$$=1+\prod_{i=1}^{2}\sum_{j\geq r_i+1}\prod_{i=r_i+1}^{j}\left[\frac{1+\sum_{k=1}^{\infty}\left[\left(C_k+8Ti^{-2}\right)\exp\left[-4C_k^{-1}Ti^{-2}\right]-2\left(C_k+8T(i+1)^{-2}\right)\exp\left[-4C_k^{-1}T(i+1)^{-2}\right]\right]}{1-\sum_{k=1}^{\infty}\left[\left(C_k+8T(i+1)^{-2}\right)\exp\left[-4C_k^{-1}T(i+1)^{-2}\right]\right]}\right]. \quad (3.10)$$

When $r=0$, then

$$\mu_{R_1(T),R_2(T)}(0,0;T)=\left(\frac{L_{R_1(T),R_2(T)}(0,0;T)}{1-\sum_{k=1}^{\infty}\left(\frac{8}{(2k-1)^2\pi^2}+8T\right)\exp\left[-\frac{(2k-1)^2\pi^2T}{2}\right]}\right)^2. \quad (3.11)$$

The mean residual life function of a discrete multivariate distribution is an important analysis measure for calculating the expected value of the remaining price variation after a designated amount is attained within a limited price range. For the distribution of ranges of the Wiener process, the function is utilized to estimate the mean length or lag of prices remaining within the lower and higher limits such that the stability of prices can be assessed, and whether there is a likelihood of an ongoing trend continuing can be ascertained. Barlow and Proschan [27] pointed out that this function is a fundamental tool in reliability models, as it reflects the temporal characteristics of the system or asset under study. This can be translated in financial contexts into an analysis of the risk of the price remaining in a certain region before a significant change occurs.

Remark 2. In this context, the standard hazard rate is forward looking and quantifies the conditional probability of observing a given range value given the survival beyond it. In contrast, the reversed hazard rate is backward looking and describes the likelihood that the range has already reached a given level. The second failure rate captures the cumulative evolution of risk and reflects how risk builds up as the range increases.

The reversed hazard rate function is an important measure of analysis in the multivariate discrete distribution of the Wiener process, specifically in the study of stock price motions in a finite price range. The function is different from the conventional hazard function as it focuses on estimating the probability that a price movement will be observed up to a point in time and, thus, comes into play in studies on backward looking risk and pre-exceedance behavior. Thus, the joint reversed hazard rate function of the this distribution is given by,

$$RH_{R_1(T),R_2(T)}(r_1,r_2;T)=\prod_{i=1}^{2}P[(R_i(T)=r_i)/(R_i(T)\leq r_i)]=\prod_{i=1}^{2}\left(\frac{P[R_i(T)=r_i]}{P[R_i(T)\leq r_i]}\right)$$

$$=\prod_{i=1}^{2}\left(\frac{\sum_{k=1}^{\infty}\left[\left(C_k+8T(r_i+1)^{-2}\right)\exp\left[-4C_k^{-1}T(r_i+1)^{-2}\right]-\left(C_k+8Tr_i^{-2}\right)\exp\left[-4C_k^{-1}Tr_i^{-2}\right]\right]}{\sum_{k=1}^{\infty}\left[\left(C_k+8T(r_i+1)^{-2}\right)\exp\left[-4C_k^{-1}T(r_i+1)^{-2}\right]\right]}\right). \quad (3.12)$$

Samaniego [30] demonstrated that such a function is used in an effort to determine historical dependence and determine previous events, which is relevant in the event of markets with price upper and lower bounds. Thus, in the truncated case, the joint truncated reversed hazard rate function of the this distribution is,

$$R\bar{H}_{\bar{R}_1(T),\bar{R}_2(T)}(\bar{r}_1,\bar{r}_2;T)=\frac{\bar{f}_{\bar{R}_1(T),\bar{R}_2(T)}(\bar{r}_1,\bar{r}_2;T)}{\{\bar{F}_{\bar{R}_1(T),\bar{R}_2(T)}(\bar{r}_1,\bar{r}_2;T)\}^{-1}}$$

$$=\prod_{i=1}^{2}\left(\frac{\sum_{k=1}^{\infty}\left[\left(C_k+8T(\bar{r}_i+1)^{-2}\right)\exp\left[-4C_k^{-1}T(\bar{r}_i+1)^{-2}\right]-\left(C_k+8T\bar{r}_i^{-2}\right)\exp\left[-4C_k^{-1}T\bar{r}_i^{-2}\right]\right]}{\sum_{k=1}^{\infty}\left[\left(C_k+8T(\bar{r}_i+1)^{-2}\right)\exp\left[-4C_k^{-1}T(\bar{r}_i+1)^{-2}\right]-\left(C_k+8T(a_i+1)^{-2}\right)\exp\left[-4C_k^{-1}Ta_i^{-2}\right]\right]}\right). \quad (3.13)$$

Figures 9 and 10 demonstrate the transition from the continuous to the discrete joint reversed hazard rate function for both the original and truncated distributions, respectively.

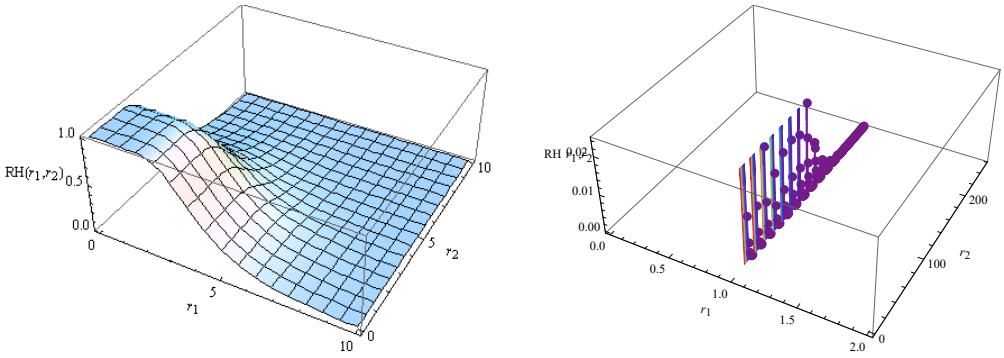

(a) **(b)**

Figure 9. The joint bivariate reversed hazard rate function **(a)** continuous case; and **(b)** discrete case.

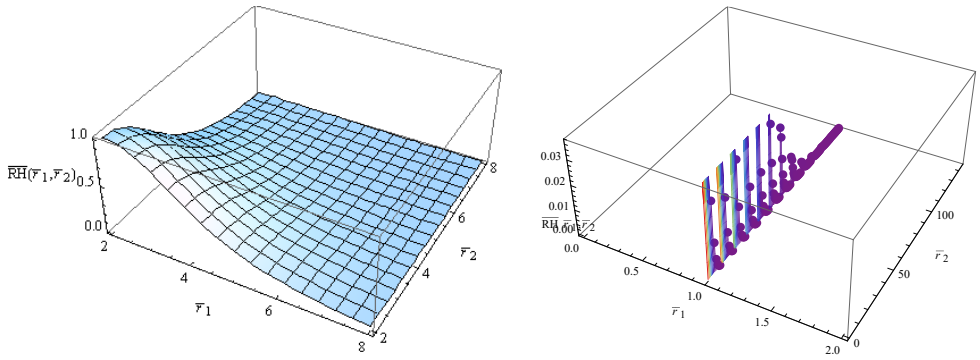

(a) **(b)**

Figure 10. The joint bivariate truncated reversed hazard rate function **(a)** continuous case; and **(b)** discrete case.

The second rate of failure function of a discrete multivariate distribution is used to model how risk evolves with time. It is a useful method for examining the dynamic pattern of the behavior of stock price movement, particularly for markets with upper and lower price limits. In the framework of the Wiener process range distribution, the function enables the analysis of the buildup of the probability of large price movements after reaching certain levels, providing advanced information on the timing and risk buildup. It is utilized as well to calculate cumulative risk and analyze the dynamics of price volatility in a discrete and truncated distribution framework, providing support for quantitative models in constrained financial markets. Using the method that devolved in [13], we

obtain the joint second rate of failure function by,

$$SH_{R_1(T),R_2(T)}(r_1, r_2; T) = \prod_{i=1}^{2}\left(log\left\{\frac{S_{R_i(T)}(r_i)]}{S_{R_i(T)}(r_i+1)}\right\}\right).$$

On the other hand, the joint truncated version of this function is used to analyze the change in price risk within a bounded range, which helps understand the dynamics of asset price volatility as it approaches upper and lower bounds over a specific time period. Additionally, the joint truncated second rate of failure function is given from,

$$S\bar{H}_{\bar{R}_1(T),\bar{R}_2(T)}(\bar{r}_1, \bar{r}_2; T) = \prod_{i=1}^{2}\left(log\left\{\frac{\bar{S}_{\bar{R}_i(T)}(\bar{r}_i)]}{\bar{S}_{\bar{R}_i(T)}(\bar{r}_i+1)}\right\}\right).$$

Figures 11 and 12 depict the transition from the continuous to the discrete joint second rate of failure function for both the original and truncated distributions, respectively.

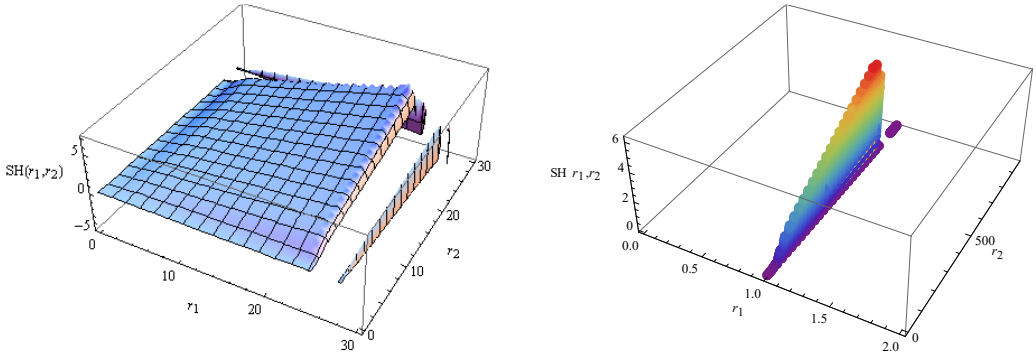

(a) **(b)**

Figure 11. The joint bivariate second rate of failure function **(a)** continuous case; and **(b)** discrete case.

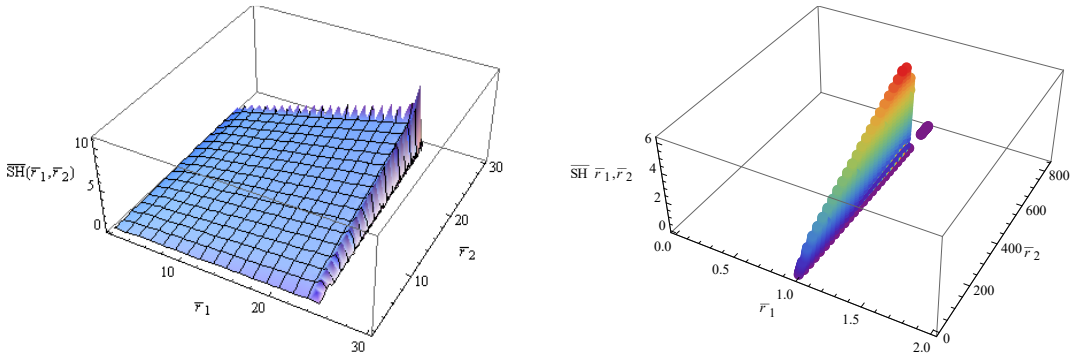

(a) **(b)**

Figure 12. The joint bivariate truncated second rate of failure function **(a)** continuous case; and **(b)** discrete case.

3.2. *Moments*

Moments about the origin are inherent properties in identifying the statistical behavior of the multivariate discrete distribution of the Wiener process range, specifically in analyzing stock price

movements within a finite price boundary. They record parameters such as mean, first and second order variance, central tendency, and probability dispersion of the price movement. These measures are utilized to interpret direction in the market, stability of price, and quantify underlying risk. As Kotz et al. [31] demonstrated, such instances near the beginning are invaluable aides in the study of non-conventional distributions, especially in price restricted environments that require discrete form multivariate models. From a computational perspective, the evaluation of multivariate discrete moments is commonly carried out using series representations closely related to probability generating functions (PGFs). In such settings, exact closed-form expressions are rarely available, and numerical evaluation relies on controlled truncation of infinite series with guaranteed convergence properties. Standard references on discrete multivariate distributions and generating-function methods provide the theoretical justification for this approach, including convergence control and truncation accuracy [32–34].

In the multivariate case, the joint moment about the origin is defined using a multi-index notation. Specifically, let $\boldsymbol{q} = [q_1, q_2, ..., q_n] \in \mathbf{N}_0^n$ be a vector of non-negative integers, where $\mathbf{N}_0^n$ denotes the set of all n-dimensional vectors with non-negative integer components. Then, the joint $\boldsymbol{q^{th}}$ moment about the origin of the random vector $[R_1(T), R_2(T), \ldots, R_n(T)]$ is then defined by,

$$\mu'_{\boldsymbol{q}} = E\left[\prod_{i=1}^{n} (R_i(T))^{q_i}\right].$$

This definition clarifies that each component $R_i(T)$ is raised to its corresponding power q_i. Thus, for the original distribution, Eq (3.14) below is formulated according to this standard multivariate moment definition as follows:

$$\mu'_{q_1}\mu'_{q_2}...\mu'_{q_n} = \prod_{i=1}^{n}\sum_{r_i=0}^{\infty}\left[r_i^{q_i}\sum_{k=1}^{\infty}\left[\left(C_k + 8T(r_i+1)^{-2}\right)\exp\left[-4C_kT(r_i+1)^{-2}\right] - \left(C_k + 8Tr_i^{-2}\right)\exp\left[-4C_kTr_i^{-2}\right]\right]\right]. \quad (3.14)$$

For a truncated case, the joint q^{th} moment of $[\bar{R}_1(T), \bar{R}_2(T), \ldots, \bar{R}_n(T)]$ about the origin is,

$$\bar{\mu}'_{q_1}\bar{\mu}'_{q_2}...\bar{\mu}'_{q_n} = \prod_{i=1}^{n}\sum_{\bar{r}_i=0}^{\infty}\left[\frac{\bar{r}_i^{q_i}\sum_{k=1}^{\infty}\left[\left(C_k + 8T(\bar{r}_i+1)^{-2}\right)\exp\left[-4C_k^{-1}T(\bar{r}_i+1)^{-2}\right] - \left(C_k + 8T\bar{r}_i^{-2}\right)\exp\left[-4C_k^{-1}T\bar{r}_i^{-2}\right]\right]}{\sum_{k=1}^{\infty}\left[\left(C_k + 8T(b_i+1)^{-2}\right)\exp\left[-4C_k^{-1}T(b_i+1)^{-2}\right]\right] - \sum_{k=1}^{\infty}\left[\left(C_k + 8T(a_i+1)^{-2}\right)\exp\left[-4C_k^{-1}T(a_i+1)^{-2}\right]\right]}\right]. \quad (3.15)$$

The exact evaluation of the above moments is analytically challenging; however, they can be computed numerically. Since the analytical evaluation of the joint moments involves infinite series, all numerical computations are carried out using truncated sums. The series terms decay exponentially due to the factor $\exp[-4C_kT]$, ensuring rapid convergence. In practice, truncation at moderate upper indices is sufficient, as numerical stability is achieved, and further increases in the truncation level do not affect the computed moments.

3.3. *Order statistics*

Order statistics are important in discrete multivariate distribution theory, especially in Wiener process range distribution theory of differences between upper and lower price limits of stock prices.

They are used for maximum and minimum value identification and internal ranking of samples, which help in analyzing price behavior at the extremes or when close to price stops. They are particularly handy in models that attempt to describe the relationship between the upper and lower bounds of a stock price within a time horizon. David and Nagaraja [35] averred that order statistics play a key role in relative performance measurement of assets and marginal and conditional probability estimation, especially in non-standard or discrete multivariate distributions.

Let $R_{i1}, R_{i2}, \ldots, R_{i\tilde{n}}, i = 1,2,\ldots,n$ be a random sample of independent and identically distributed discrete random variables, each representing the discretized range of an independent Wiener process over the time interval $(0,T)$. Denote by $R_{(1:\tilde{n})} \leq R_{(2:\tilde{n})} \leq \ldots \leq R_{(\tilde{n}:\tilde{n})}$ the corresponding order statistics obtained by arranging the sample in nondecreasing order. Here, $R_{(p:\tilde{n})}$ represents the p^{th} order statistic, that is, the p^{th} smallest observed range among the n components. Accordingly, let

$$\left[R_{1(1:\tilde{n})}, R_{1(2:\tilde{n})}, \ldots, R_{1(\tilde{n}:\tilde{n})}\right] \leq \left[R_{2(1:\tilde{n})}, R_{2(2:\tilde{n})}, \ldots, R_{2(\tilde{n}:\tilde{n})}\right] \leq \ldots \leq \left[R_{n(1:\tilde{n})}, R_{n(2:\tilde{n})}, \ldots, R_{n(\tilde{n}:\tilde{n})}\right]$$

denote the order statistics of $R_{i1}, R_{i2}, \ldots, R_{i\tilde{n}}$, then under the assumption of independence, the joint PMF of the p_i^{th} order statistic $R_{i(p_i:\tilde{n})}$, $i = 1,2,\ldots,n$ is,

$$\begin{aligned}
&\widetilde{f}_{R_1(T),R_2(T),\ldots,R_n(T)(p_1:\tilde{n},p_2:\tilde{n},\ldots,p_n:\tilde{n})}(r_1,r_2,\ldots,r_n;T) = \prod_{i=1}^{n}\left[\frac{\tilde{n}!}{(p_i-1)!(\tilde{n}-p_i)!}\left(F_{R_i(T)}(r_i)\right)^{p_i-1}\left(1-F_{R_i(T)}(r_i)\right)^{\tilde{n}-p_i} f_{R_i(T)}(r_i)\right] \\
&= \prod_{i=1}^{n}\left[\frac{\tilde{n}!}{(p_i-1)!(\tilde{n}-p_i)!}\left(\sum_{k=1}^{\infty}\left[\left(C_k+8T(r_i+1)^{-2}\right)\exp\left[-4C_kT(r_i+1)^{-2}\right]\right]\right)^{p_i-1}\right. \\
&\cdot\left(1-\sum_{k=1}^{\infty}\left[\left(C_k+8T(r_i+1)^{-2}\right)\exp\left[-4C_kT(r_i+1)^{-2}\right]\right]\right)^{\tilde{n}-p_i} \\
&\left.\cdot\left(\sum_{k=1}^{\infty}\left[\left(C_k+8T(r_i+1)^{-2}\right)\exp\left[-4C_kT(r_i+1)^{-2}\right]-\left(C_k+8Tr_i^{-2}\right)\exp\left[-4C_kTr_i^{-2}\right]\right]\right)\right]. \qquad (3.16)
\end{aligned}$$

The joint distribution of discrete order statistics in (3.16) is obtained using the standard distribution function approach under the assumption of independent and identically distributed components. Since these derivations follow classical and well-established results in discrete order statistics theory, the detailed algebra is omitted for brevity. Interested readers are referred to [32,35,36] for comprehensive derivations and theoretical background.

In addition, the joint CDF of the random vector $\left[R_{1(p_1:\tilde{n})}, R_{2(p_2:\tilde{n})}, \ldots, R_{n(p_n:\tilde{n})}\right]$ is,

$$\begin{aligned}
&\widetilde{F}_{R_1(T),R_2(T),\ldots,R_n(T)(p_1:\tilde{n},p_2:\tilde{n},\ldots,p_n:\tilde{n})}(r_1,r_2,\ldots,r_n;T) = \prod_{i=1}^{n}\sum_{\tilde{i}=p}^{\tilde{n}}\binom{\tilde{n}}{\tilde{i}}\left(F_{R_i(T)}(r_i)\right)^{\tilde{i}}\left(1-F_{R_i(T)}(r_i)\right)^{\tilde{n}-\tilde{i}} \qquad (3.17) \\
&= \prod_{i=1}^{n}\sum_{\tilde{i}=p_i}^{\tilde{n}}\binom{\tilde{n}}{\tilde{i}}\left(\sum_{k=1}^{\infty}\left[\left(C_k+8T(r_i+1)^{-2}\right)\exp\left[-4C_kT(r_i+1)^{-2}\right]\right]\right)^{\tilde{i}} \\
&\cdot\left(1-\sum_{k=1}^{\infty}\left[\left(C_k+8T(r_i+1)^{-2}\right)\exp\left[-4C_kT(r_i+1)^{-2}\right]\right]\right)^{\tilde{n}-\tilde{i}}.
\end{aligned}$$

Additionally, the joint PMF of minimum price changes is a fundamental tool for modeling cases where the minimum price change is the primary determinant of the behavior of a financial asset.

Within the framework of the discrete multivariate distribution of the Wiener process range, this function enables one to give an exact description of the probability of minimum price movements on various components (e.g., various assets or time periods), within a set of prices bounded from above and below. This type of analysis is important in applications focused on estimating minimum risks or price inertia. Balakrishnan and Nevzorov [37] pointed out that the analysis of minimum order statistics in discrete distributions is essential for assessing reliability and probability concentration in constrained markets, especially when using models belonging to the class of stochastic processes associated with the Wiener process. At a knowing time T, this function is given by,

$$\hat{f}_{(R_1(T),R_2(T),\ldots,R_n(T))(1:\tilde{n})}(r_1,r_2,\ldots,r_n;T)=\prod_{i=1}^{n}\left[\tilde{n}\left(1-\sum_{k=1}^{\infty}\left[\left(C_k+8T(r_i+1)^{-2}\right)\exp\left[-4C_kT(r_i+1)^{-2}\right]\right]\right)^{\tilde{n}-1}\right. \tag{3.18}$$
$$\left.\cdot\left(\sum_{k=1}^{\infty}\left[\left(C_k+8T(r_i+1)^{-2}\right)\exp\left[-4C_kT(r_i+1)^{-2}\right]-\left(C_k+8Tr_i^{-2}\right)\exp\left[-4C_kTr_i^{-2}\right]\right]\right)\right].$$

Equation (3.18) follows directly from the general expression in Eq (3.16) by setting $p=1$, which corresponds to the minimum order statistic, that is, the smallest observed discrete Wiener process range among the n components.

On the other hand, the joint probability mass function of the largest price difference in the discrete multivariate distribution of the Wiener process range is used to analyze the probability of extreme fluctuations within specific price ranges, which helps in assessing marginal risks and estimating the chances of prices breaking through their extreme ranges. This function is given by,

$$\tilde{f}_{(R_1(T),R_2(T),\ldots,R_n(T))(\tilde{n}:\tilde{n})}(r_1,r_2,\ldots,r_n;T)=\prod_{i=1}^{n}\left[\tilde{n}\left(\sum_{k=1}^{\infty}\left[\left(C_k+8T(r_i+1)^{-2}\right)\exp\left[-4C_kT(r_i+1)^{-2}\right]\right]\right)^{\tilde{n}-1}\right. \tag{3.19}$$
$$\left.\cdot\left(\sum_{k=1}^{\infty}\left[\left(C_k+8T(r_i+1)^{-2}\right)\exp\left[-4C_kT(r_i+1)^{-2}\right]-\left(C_k+8Tr_i^{-2}\right)\exp\left[-4C_kTr_i^{-2}\right]\right]\right)\right].$$

Determining the probability of reaching maximum or minimum values within a specific data set over a given period requires finding these statistics for the truncated distribution. These probabilities help characterize the marginal behavior of prices, the statistics enhance the accuracy of edge risk assessment and provide a quantitative framework for analyzing the relative performance of assets in markets subject to regulatory restrictions on price change. Thus, if

$$\left[\overline{R}_{1(1:m)},\overline{R}_{1(2:m)},\ldots,\overline{R}_{1(m:m)}\right]\le\left[\overline{R}_{2(1:m)},\overline{R}_{2(2:m)},\ldots,\overline{R}_{2(m:m)}\right]\le\cdots\le\left[\overline{R}_{n(1:m)},\overline{R}_{n(2:m)},\ldots,\overline{R}_{n(m:m)}\right]$$

denote to the order statistics of a random sample $\overline{R}_{i1},\overline{R}_{i2},\ldots,\overline{R}_{im}, i=1,2,\ldots,n$, then a truncated joint PMF of the jth order statistic $R_{i(j:m)},\ i=1,2,\ldots,n$ is,

$$q_{(\overline{R}_1(T),\overline{R}_2(T),\ldots,\overline{R}_m(T))(j:m)}(\overline{r}_1,\overline{r}_2,\ldots,\overline{r}_m;T)=\prod_{i=1}^{n}\frac{m!}{(j-1)!(m-j)!}\left(\overline{F}_{\overline{R}_i(T)}(\overline{r}_i)\right)^{j-1}\left(1-\overline{F}_{\overline{R}_i(T)}(\overline{r}_i)\right)^{m-j}\bar{f}_{\overline{R}_i(T)}(\overline{r}_i) \tag{3.20}$$
$$=\frac{m!}{(j-1)!(m-j)!}\prod_{i=1}^{n}\left(\frac{\sum_{k=1}^{\infty}\left[\left(C_k+8T(\overline{r}_i+1)^{-2}\right)\exp\left[-4C_k^{-1}T(\overline{r}_i+1)^{-2}\right]-\left(C_k+8T(a_i+1)^{-2}\right)\exp\left[-4C_k^{-1}T(a_i+1)^{-2}\right]\right]}{\sum_{k=1}^{\infty}\left[\left(C_k+8T(b_i+1)^{-2}\right)\exp\left[-4C_k^{-1}T(b_i+1)^{-2}\right]-\left(C_k+8T(a_i+1)^{-2}\right)\exp\left[-4C_k^{-1}T(a_i+1)^{-2}\right]\right]}\right)^{j-1}$$

$$\cdot\left(1-\frac{\sum_{k=1}^{\infty}\left[\left(C_k+8T(\bar{r}_i+1)^{-2}\right)\exp\left[-4C_k^{-1}T(\bar{r}_i+1)^{-2}\right]-\left(C_k+8T(a_i+1)^{-2}\right)\exp\left[-4C_k^{-1}T(a_i+1)^{-2}\right]\right]}{\sum_{k=1}^{\infty}\left[\left(C_k+8T(b_i+1)^{-2}\right)\exp\left[-4C_k^{-1}T(b_i+1)^{-2}\right]-\left(C_k+8T(a_i+1)^{-2}\right)\exp\left[-4C_k^{-1}T(a_i+1)^{-2}\right]\right]}\right)^{m-j}$$

$$\cdot\left(\frac{\sum_{k=1}^{\infty}\left[\left(C_k+8T(\bar{r}_i+1)^{-2}\right)\exp\left[-4C_k^{-1}T(\bar{r}_i+1)^{-2}\right]-\left(C_k+8T\bar{r}_i^{-2}\right)\exp\left[-4C_k^{-1}T\bar{r}_i^{-2}\right]\right]}{\sum_{k=1}^{\infty}\left[\left(C_k+8T(b_i+1)^{-2}\right)\exp\left[-4C_k^{-1}T(b_i+1)^{-2}\right]-\sum_{k=1}^{\infty}\left[\left(C_k+8T(a_i+1)^{-2}\right)\exp\left[-4C_k^{-1}T(a_i+1)^{-2}\right]\right]}\right).$$

Additionally, a truncated joint CDF of $\bar{R}_{i1},\bar{R}_{i2},\ldots,\bar{R}_{im}, i=1,2,\ldots,n$ is,

$$Q_{(\bar{R}_1(T),\bar{R}_2(T),\ldots,\bar{R}_m(T))(j:m)}(\bar{r}_1,\bar{r}_2,\ldots,\bar{r}_m;T)=\prod_{i=1}^{n}\sum_{\tilde{i}=j}^{m}\binom{m}{\tilde{i}}\left(\overline{F}_{\bar{R}_i(T)}(\bar{r}_i)\right)^{\tilde{i}}\left(1-\overline{F}_{\bar{R}_i(T)}(\bar{r}_i)\right)^{m-\tilde{i}} \tag{3.21}$$

$$=\prod_{i=1}^{n}\sum_{\tilde{i}=j}^{m}\binom{m}{\tilde{i}}\left(\frac{\sum_{k=1}^{\infty}\left[\left(C_k+8T(\bar{r}_i+1)^{-2}\right)\exp\left[-4C_k^{-1}T(\bar{r}_i+1)^{-2}\right]-\left(C_k+8T(a_i+1)^{-2}\right)\exp\left[-4C_k^{-1}T(a_i+1)^{-2}\right]\right]}{\sum_{k=1}^{\infty}\left[\left(C_k+8T(b_i+1)^{-2}\right)\exp\left[-4C_k^{-1}T(b_i+1)^{-2}\right]-\left(C_k+8T(a_i+1)^{-2}\right)\exp\left[-4C_k^{-1}T(a_i+1)^{-2}\right]\right]}\right)^{\tilde{i}}$$

$$\cdot\left(1-\frac{\sum_{k=1}^{\infty}\left[\left(C_k+8T(\bar{r}_i+1)^{-2}\right)\exp\left[-4C_k^{-1}T(\bar{r}_i+1)^{-2}\right]-\left(C_k+8T(a_i+1)^{-2}\right)\exp\left[-4C_k^{-1}T(a_i+1)^{-2}\right]\right]}{\sum_{k=1}^{\infty}\left[\left(C_k+8T(b_i+1)^{-2}\right)\exp\left[-4C_k^{-1}T(b_i+1)^{-2}\right]-\left(C_k+8T(a_i+1)^{-2}\right)\exp\left[-4C_k^{-1}T(a_i+1)^{-2}\right]\right]}\right)^{m-\tilde{i}}.$$

The two truncated joint probability functions for the maximum and minimum spreads are powerful tools for characterizing extreme and local changes in asset prices within a specified price range. This representation contributes to supporting probabilistic measurement models for maximum and minimum spreads in a realistic financial environment based on the multivariate, discrete Weiner distribution. The joint truncated PMF of the minimum and maximum differences between the prices at knowing time T are given by:

$$\hat{q}_{(\bar{R}_1(T),\bar{R}_2(T),\ldots,\bar{R}_m(T))(1:m)}(\bar{r}_1,\bar{r}_2,\ldots,\bar{r}_m;T)=$$

$$m.\prod_{i=1}^{n}\left(1-\frac{\sum_{k=1}^{\infty}\left[\left(C_k+8T(\bar{r}_i+1)^{-2}\right)\exp\left[-4C_k^{-1}T(\bar{r}_i+1)^{-2}\right]-\left(C_k+8T(a_i+1)^{-2}\right)\exp\left[-4C_k^{-1}T(a_i+1)^{-2}\right]\right]}{\sum_{k=1}^{\infty}\left[\left(C_k+8T(b_i+1)^{-2}\right)\exp\left[-4C_k^{-1}T(b_i+1)^{-2}\right]-\left(C_k+8T(a_i+1)^{-2}\right)\exp\left[-4C_k^{-1}T(a_i+1)^{-2}\right]\right]}\right)^{m-1}$$

$$\cdot\left(\frac{\sum_{k=1}^{\infty}\left[\left(C_k+8T(\bar{r}_i+1)^{-2}\right)\exp\left[-4C_k^{-1}T(\bar{r}_i+1)^{-2}\right]-\left(C_k+8T\bar{r}_i^{-2}\right)\exp\left[-4C_k^{-1}T\bar{r}_i^{-2}\right]\right]}{\sum_{k=1}^{\infty}\left[\left(C_k+8T(b_i+1)^{-2}\right)\exp\left[-4C_k^{-1}T(b_i+1)^{-2}\right]-\left(C_k+8T(a_i+1)^{-2}\right)\exp\left[-4C_k^{-1}T(a_i+1)^{-2}\right]\right]}\right); \tag{3.22}$$

and

$$\widetilde{q}_{(\bar{R}_1(T),\bar{R}_2(T),\ldots,\bar{R}_m(T))(m:m)}(\bar{r}_1,\bar{r}_2,\ldots,\bar{r}_m;T) =$$

$$m\prod_{i=1}^{n}\left(\frac{\sum_{k=1}^{\infty}\left[\left(C_k+8T(\bar{r}_i+1)^{-2}\right)\exp\left[-4C_k^{-1}T(\bar{r}_i+1)^{-2}\right]-\left(C_k+8T(a_i+1)^{-2}\right)\exp\left[-4C_k^{-1}T(a_i+1)^{-2}\right]\right]}{\sum_{k=1}^{\infty}\left[\left(C_k+8T(b_i+1)^{-2}\right)\exp\left[-4C_k^{-1}T(b_i+1)^{-2}\right]-\left(C_k+8T(a_i+1)^{-2}\right)\exp\left[-4C_k^{-1}T(a_i+1)^{-2}\right]\right]}\right)^{m-1}$$

$$\cdot\left(\frac{\sum_{k=1}^{\infty}\left[\left(C_k+8T(\bar{r}_i+1)^{-2}\right)\exp\left[-4C_k^{-1}T(\bar{r}_i+1)^{-2}\right]-\left(C_k+8T\bar{r}_i^{-2}\right)\exp\left[-4C_k^{-1}T\bar{r}_i^{-2}\right]\right]}{\sum_{k=1}^{\infty}\left[\left(C_k+8T(b_i+1)^{-2}\right)\exp\left[-4C_k^{-1}T(b_i+1)^{-2}\right]-\left(C_k+8T(a_i+1)^{-2}\right)\exp\left[-4C_k^{-1}T(a_i+1)^{-2}\right]\right]}\right), \tag{3.23}$$

respectively.

3.4. *Stress-strength parameter*

The stress-strength parameter is an important probability measure in the discrete multivariate distribution of the Wiener process range. It is used to estimate the probability that one component of price change (strength) will outperform another (stress) within a confined price range. This is a highly applicable concept in price-limited financial markets, as it characterizes the asset behavior in the cases of crossover or extreme price divergence. This parameter, according to the literature, e.g., Kotz et al. [38], has a variety of applications in reliability theory and in the assessment of relative asset performance; and hence, it is a highly useful analytical instrument for relative risk assessment in truncated multivariate discrete distribution-based models. If the random variable vector $\left[R_1(T),R_2(T),\ldots,R_n(T)\right]$ for the variation of stock price is the strength of an element placed on a random stress vector $\left[Z,Z_2,\ldots,Z_n\right]$, then the model for stress-strength is,

$$P([R_1(T),R_2(T),\ldots,R_n(T)]>[Z_1,Z_2,\ldots,Z_n])=\prod_{i=1}^{n}\sum_{r_i=0}^{\infty}f_{R_i(T)}(r_i)\,F_{R_i(T)}(r_i).$$

We assume that $\{R_i(T)\}_{i=1\ldots n}$ and $\{Z_i\}_{i=1\ldots n}$ are mutually independent collections of independent random variables. These assumptions are standard in classical stress-strength reliability models and ensure the rigorous derivation of the multivariate discrete stress-strength parameter given by,

$$\Delta=\prod_{i=1}^{n}\sum_{r_i=0}^{\infty}\left(\sum_{k=1}^{\infty}\left[\left(C_k+8T(r_i+1)^{-2}\right)\exp\left[-4C_kT(r_i+1)^{-2}\right]-\left(C_k+8Tr_i^{-2}\right)\exp\left[-4C_kTr_i^{-2}\right]\right]\right.$$

$$\left.\cdot\sum_{k=1}^{\infty}\left[\left(C_k+8T(r_i+1)^{-2}\right)\exp\left[-4C_kT(r_i+1)^{-2}\right]\right]\right). \tag{3.24}$$

Moreover, for the truncated version of this distribution, we consider the values $r_i=a_i,\ldots,a_i+\hat{i},\ldots,b_i$, $i=1,2,\ldots,n$ ($\hat{i}$ is a non-negative real number) and describe the changing of stock price on the random variable vector $\left[\bar{R}_1(T),\bar{R}_2(T),\ldots,\bar{R}_n(T)\right]$. Therefore, when the changing of stock price is the strength of an element placed on a random stress vector $\left[\bar{Z},\bar{Z}_2,\ldots,\bar{Z}_n\right]$, then the stress-strength parameter is given by,

$$P\left(\left[\bar{R}_1(T),\bar{R}_2(T),\ldots,\bar{R}_n(T)\right]>\left[\bar{Z}_1,\bar{Z}_2,\ldots,\bar{Z}_n\right]\right)=\prod_{i=1}^{n}\sum_{\bar{r}_i=0}^{\infty}f_{\bar{R}_i(T)}(\bar{r}_i)F_{\bar{R}_i(T)}(\bar{r}_i)$$

$$= \prod_{i=1}^{n} \left(\frac{1}{\xi_{ik}^2} \sum_{\bar{r}_i=0}^{\infty} \left(\sum_{k=1}^{\infty} \left[\left(C_k + 8T(\bar{r}_i+1)^{-2} \right) \exp\left[-4C_k T(\bar{r}_i+1)^{-2} \right] - \left(C_k + 8T\bar{r}_i^{-2} \right) \exp\left[-4C_k T\bar{r}_i^{-2} \right] \right] \right. \right.$$

$$\left. \left. \cdot \sum_{k=1}^{\infty} \left[\left(C_k + 8T(\bar{r}_i+1)^{-2} \right) \exp\left[-4C_k T(\bar{r}_i+1)^{-2} \right] - \left(C_k + (a_i+1)^{-2} \right) \exp\left[-4C_k T(a_i+1)^{-2} \right] \right] \right) \right),$$

where,

$$\xi_{ik} = \sum_{k=1}^{\infty} \left[\left(C_k + (b_i+1)^{-2} \right) \exp\left[-4C_k T(b_i+1)^{-2} \right] - \left(C_k + (a_i+1)^{-2} \right) \exp\left[-4C_k T(a_i+1)^{-2} \right] \right].$$

4. Applications

To demonstrate the practical application of the proposed discrete multivariate Wiener process range distribution in constrained financial markets, we simulate a scenario involving two independent real world stocks: Apple Inc. (AAPL) and Microsoft Corp. It should be emphasized that the Wiener process framework adopted in this empirical illustration is used purely as a modeling approximation. The Wiener process assumption is adopted here as a standard modeling approximation commonly used in financial time series analysis [23]. No formal statistical validation of the Brownian motion assumption is conducted for the AAPL and MSFT high-low range data considered here. Our purpose of this section is to illustrate the practical implementation and interpretability of the proposed discrete multivariate Wiener range distribution, rather than to empirically verify the underlying diffusion assumption. Both AAPL and MSFT are traded on the NASDAQ stock exchange and are two of the most heavily traded technology companies in the world. These two stocks have high liquidity, huge market capitalization, and daily price movements that can be modeled within bounded range assumptions. In this empirical illustration, the independence assumption between AAPL and MSFT is adopted for methodological clarity to validate the baseline behavior of the proposed discrete bivariate Wiener range distribution. This assumption enables isolating the intrinsic probabilistic characteristics of the model. In future extensions, this restriction can be relaxed by introducing dependence structures through dynamic copula models to capture realistic cross asset correlations.

Specifically, we assume a market condition in which the high and low price ranges of each stock are bounded, with Microsoft constrained in the interval $[2,8]$ units and Apple in the interval $[1,7]$ units, reflecting bounded price movement mechanisms imposed for illustrative modeling purposes. A real dataset of hourly high-low price ranges is obtained from publicly available financial data sources (e.g., NASDAQ via Alpha Vantage API (source of data: https://www.alphavantage.co/)) and processed across discrete time intervals, as shown in Table 1. This data is restricted in the ranges $\bar{r}_1 \in [2,8]$, and $\bar{r}_2 \in [1,7]$, and the time interval $T=1$.

Remark 3. The truncation intervals $[2,8]$ for MSFT and $[1,7]$ for AAPL are adopted for illustrative purposes only. They are not claimed to represent empirically estimated market specific bounds, nor are they intended to characterize emerging market mechanisms for the assets considered. Instead, these intervals are chosen to lie within the empirically observed range of the high-low data and may be viewed as approximating interior empirical quantiles of the sample. This choice enables a clear demonstration of the effect of truncation on the proposed distribution while maintaining consistency with the observed data.

Table 1. Hourly Trading Data for Microsoft (MSFT) and Apple (AAPL) with High-Low price range differences.

Timestamp	MSFT High	MSFT LOW	$\bar{r}_1$	AAPL High	AAPL Low	$\bar{r}_2$
2025-08-24 07:24:26	340.61	335.22	5.39	177.15	175.02	2.13
2025-08-24 08:24:26	339.17	336.79	2.38	177.98	173.58	4.4
2025-08-24 09:24:26	340.6	335.27	5.33	176.12	174.89	1.23
2025-08-24 10:24:26	340.38	333.49	6.89	177.75	173.21	4.54
2025-08-24 11:24:26	340.5	334.27	6.23	176.16	174.16	2
2025-08-24 12:24:26	342.1	335.28	6.82	177.19	172.12	5.07
2025-08-24 13:24:26	340.29	335.31	4.98	175.04	173.91	1.13
2025-08-24 14:24:26	342.53	335.24	7.29	175.29	172.43	2.86
2025-08-24 15:24:26	339.8	337.15	2.65	176.4	169.77	6.63
2025-08-24 16:24:26	341.8	334.55	7.25	175.17	170.94	4.23
2025-08-24 17:24:26	340.19	335.96	4.23	176.52	170.65	5.87
2025-08-24 18:24:26	338.48	335.93	2.55	175.14	170.19	4.95
2025-08-24 19:24:26	340.84	335.12	5.72	175	170.34	4.66
2025-08-24 20:24:26	340.65	335.92	4.73	173.36	171.21	2.15
2025-08-24 21:24:26	340.11	335.54	4.57	173.92	169.47	4.45
2025-08-24 22:24:26	341.22	334.11	7.11	172.83	171.59	1.24
2025-08-24 23:24:26	338.17	335.34	2.83	174.8	168.99	5.81
2025-08-25 00:24:26	339.39	333.69	5.7	176.18	169.42	6.76
2025-08-25 01:24:26	339.35	334.87	4.48	175.39	169.27	6.12
2025-08-25 02:24:26	338.66	333.49	5.17	173.21	171.91	1.3
2025-08-25 03:24:26	338.32	333.32	5	173.94	170.91	3.03
2025-08-25 04:24:26	337.3	334.5	2.8	173.43	170.52	2.91
2025-08-25 05:24:26	339.07	334	5.07	173.16	171.48	1.68
2025-08-25 06:24:26	340.93	333.76	7.17	174.61	169.85	4.76
2025-08-25 07:24:26	338.58	335.55	3.03	175.48	169.7	5.78
2025-08-25 08:24:26	337.66	335.59	2.07	174	171.12	2.88
2025-08-25 09:24:26	338.1	335.69	2.41	175	168.82	6.18
2025-08-25 10:24:26	339.06	334.3	4.76	174.74	168.96	5.78
2025-08-25 11:24:26	340.41	332.56	7.85	172.77	171	1.77
2025-08-25 12:24:26	338.27	336	2.27	175.26	169.66	5.6
2025-08-25 13:24:26	342.13	334.18	7.95	175.06	168.76	6.3
2025-08-25 14:24:26	340.92	335.7	5.22	172.98	170.8	2.18
2025-08-25 15:24:26	339.56	336.84	2.72	173.08	168.64	4.44
2025-08-25 16:24:26	340.79	336.28	4.51	173.66	168.83	4.83
2025-08-25 17:24:26	339.03	335.79	3.24	172.93	168.27	4.66
2025-08-25 18:24:26	340.54	334.26	6.28	170.31	168.73	1.58
2025-08-25 19:24:26	339.38	334.13	5.25	171.96	166.99	4.97
2025-08-25 20:24:26	340.06	336.33	3.73	172.54	167.75	4.79
2025-08-25 21:24:26	340.39	336.86	3.53	172.2	166.26	5.94
2025-08-25 22:24:26	342.31	335.11	7.2	171.49	165.67	5.82
2025-08-25 23:24:26	341.89	335.29	6.6	169.61	166.65	2.96
2025-08-26 00:24:26	339.39	334.77	4.62	170.12	164.79	5.33
2025-08-26 01:24:26	339.73	335.3	4.43	170.78	164.58	6.2
2025-08-26 02:24:26	341.7	335.28	6.42	170.38	164.02	6.36
2025-08-26 03:24:26	341.96	334.14	7.82	167.75	165.78	1.97
2025-08-26 04:24:26	339.7	337.22	2.48	167.69	166.53	1.16
2025-08-26 05:24:26	340.37	337.42	2.95	169.11	164.21	4.9
2025-08-26 06:24:26	340.05	335.88	4.17	168.06	165.77	2.29
2025-08-26 07:24:26	341.05	336	5.05	168.53	164.15	4.38
2025-08-26 08:24:26	340.56	338.13	2.43	168.94	162.27	6.67

Table 2. The joint truncated PMF, CDF, survival and hazard rate functions of $\bar{r}_1$ and $\bar{r}_2$.

$\bar{r}_1$	$\bar{r}_2$	$\bar{f}_{\bar{R}_i(T),\bar{R}_2(T)}(\bar{r}_1,\bar{r}_2;T)$	$\bar{F}_{\bar{R}_i(T),\bar{R}_2(T)}(\bar{r}_1,\bar{r}_2;T)$	$\bar{S}_{\bar{R}_i(T),\bar{R}_2(T)}(\bar{r}_1,\bar{r}_2;T)$	$\bar{H}_{\bar{R}_i(T),\bar{R}_2(T)}(\bar{r}_1,\bar{r}_2;T)$
5.39	2.13	0.027057	0.1496	0.8504	0.031817
2.38	4.4	0.024648	0.0264	0.9736	0.025317
5.33	1.23	0.021813	0.0396	0.9604	0.022713
6.89	4.54	0.024435	0.42	0.58	0.042129
6.23	2	0.020681	0.148	0.852	0.024273
6.82	5.07	0.027967	0.5576	0.4424	0.063216
4.98	1.13	0.021514	0.0104	0.9896	0.02174
7.29	2.86	0.014152	0.282	0.718	0.019711
2.65	6.63	0.01987	0.1536	0.8464	0.023476
7.25	4.23	0.019261	0.368	0.632	0.030476
4.23	5.87	0.033205	0.2952	0.7048	0.047113
2.55	4.95	0.031612	0.0896	0.9104	0.034723
5.72	4.66	0.031685	0.3888	0.6112	0.05184
4.73	2.15	0.028896	0.1152	0.8848	0.032658
4.57	4.45	0.034001	0.2112	0.7888	0.043105
7.11	1.24	0.014869	0.0688	0.9312	0.015968
2.83	5.81	0.031225	0.1716	0.8284	0.037693
5.7	6.76	0.018513	0.7	0.3	0.061709
4.48	6.12	0.033278	0.344	0.656	0.050728
5.17	1.3	0.023767	0.06	0.94	0.025284
5	3.03	0.022008	0.2052	0.7948	0.02769
2.8	2.91	0.018122	0.068	0.932	0.019444
5.07	1.68	0.02842	0.0812	0.9188	0.030931
7.17	4.76	0.025079	0.4928	0.5072	0.049446
3.03	5.78	0.030943	0.1976	0.8024	0.038563
2.07	2.88	0.013194	0.0064	0.9936	0.013279
2.41	6.18	0.025065	0.0704	0.9296	0.026963
4.76	5.78	0.039578	0.38	0.62	0.063835
7.85	1.77	0.012364	0.1568	0.8432	0.014663
2.27	5.6	0.027499	0.0288	0.9712	0.028315
7.95	6.3	0.012543	0.92	0.08	0.156787
5.22	2.18	0.02817	0.1612	0.8388	0.033584
2.72	4.44	0.027774	0.0828	0.9172	0.030281
4.51	4.83	0.038253	0.252	0.748	0.05114
3.24	4.66	0.029069	0.1512	0.8488	0.034247
6.28	1.58	0.019263	0.0912	0.9088	0.021196
5.25	4.97	0.040062	0.4224	0.5776	0.06936
3.73	4.79	0.029461	0.1856	0.8144	0.036175
3.53	5.94	0.027638	0.252	0.748	0.03695
7.2	5.82	0.024566	0.72	0.28	0.087737
6.6	2.96	0.015175	0.288	0.712	0.021313
4.62	5.33	0.040955	0.322	0.678	0.060405
4.43	6.2	0.031544	0.342	0.658	0.047939
6.42	6.36	0.021415	0.7332	0.2668	0.080266
7.82	1.97	0.012906	0.1728	0.8272	0.015603
2.48	1.16	0.016358	0.0048	0.9952	0.016437
2.95	4.9	0.03231	0.1488	0.8512	0.037958
4.17	2.29	0.023724	0.0952	0.9048	0.02622
5.05	4.38	0.034152	0.2352	0.7648	0.044655
2.43	6.67	0.017919	0.098	0.902	0.019866

Next, we calculate the joint truncated empirical PMF, CDF, survival function, and hazard function for the observed data. The simulation results show good agreement with the theoretical structure of the truncated probability mass function, as presented in Eq (3.2), with the highest probabilities concentrated in the low to middle values of the price range, as shown in Figure 13. This Figure shows that most of the range values are concentrated in the range between 2 and 7, which is consistent with the nature of low volatility markets. This result is consistent with the literature; for example, El-Hadidy and Alfreedi [15] reported on their investigation of the endogenous truncated Wiener process range distribution, where they established that price volatility is most appropriately explained through the application of truncated models for restricted markets, and that the probability of price change is most appropriately explained in comparison to general continuous models.

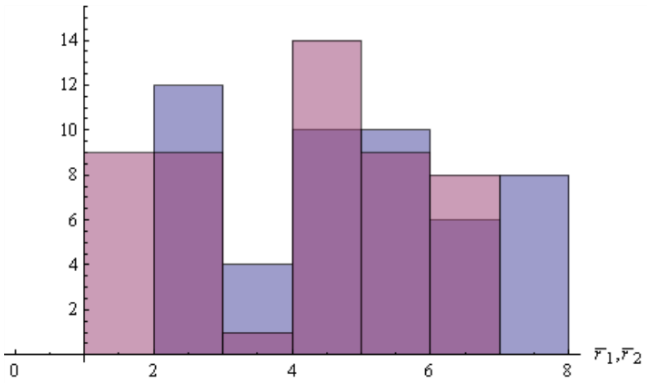

Figure 13. Histogram of simulated ranges $\bar{r}_1$ and $\bar{r}_2$.

Figure 13 also indicates that stock price difference values tend to cluster around median values, which is behavior typical of the theoretical distribution of the binary range of the discontinuous Wiener process. The natural truncation tails of the randomly generated data are also consistent with the concept of a truncated distribution achieved in Eq (3.2) of the work, with probabilities being redistributed in a restricted range. The slightly different pattern between the price differentials of the first stock, $\bar{r}_1$, and the price differentials of the second stock, $\bar{r}_2$, is also the difference in their volatilities, substantiating the use of a multivariate range distribution model over a univariate model. This model is suitable for a restricted market; however, in cases of high volatility, modification or expansion of the model may be necessary. Therefore, it is important to know the period during which stock prices are not subject to high volatility to clarify the extent of the effectiveness of our proposed model.

As shown in Figure 14, the PMF for the truncated joint is greatest at $(\bar{r}_1, \bar{r}_2) = (2,5)$ and $(4,6)$, implying that it is most likely to have co-occurring range values are in the interior of the admissible region, which agrees with moderate price volatility in the presence of market constraints. The probability mass is packed in these middle ranges and declines toward the boundaries, which suggests the effect of truncation imposed by price movement constraints and fits the regime of clustering in Figure 13. Figure 15 also illustrates the way cumulative probabilities increase steadily as $\bar{r}_1$ and $\bar{r}_2$ increase, which strongly establishes that mid-range values hold most of the probability mass.

Figure 16 shows the truncated joint survival function, which illustrates the probability that price fluctuations will exceed certain limits. We observe that the function declines steeply as the values increase, so the likelihood of highly large fluctuations is low because market constraints are imposed. This is an explicit measure of constrained markets' properties, where large fluctuations are prevented.

Therefore, such a function is very important in analyzing the risk of exposure to volatility in investment portfolios, especially in extreme cases. The estimated truncated hazard function shows an increasing pattern with increasing range values, as in Figure 17, indicating a higher risk of severe fluctuations the closer the price approaches the imposed limits.

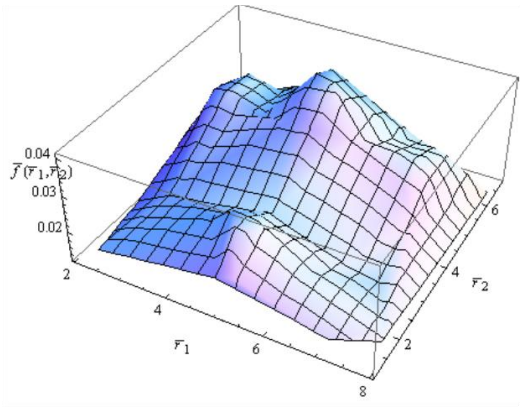

Figure 14. Truncated Joint PMF of $\bar{r}_1$ and $\bar{r}_2$.

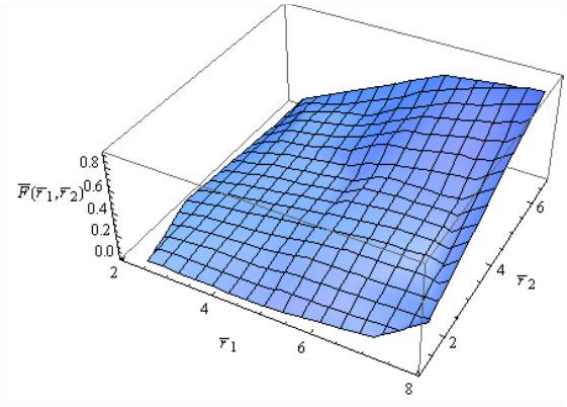

Figure 15. Truncated Joint CDF with probability values accumulate incrementally as the values of $\bar{r}_1$ and $\bar{r}_2$ increase.

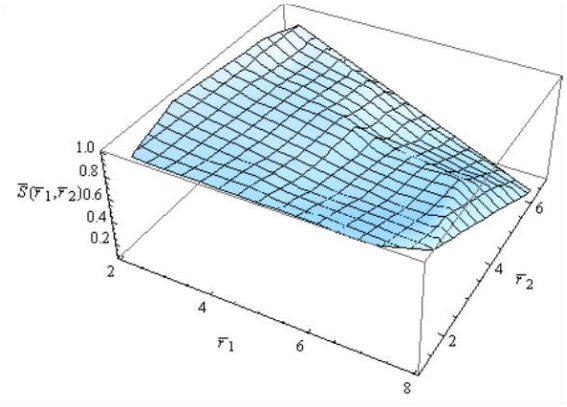

Figure 16. Truncated Joint survival function that represents the probability that the values $\bar{r}_1$ and $\bar{r}_2$ exceed certain limits.

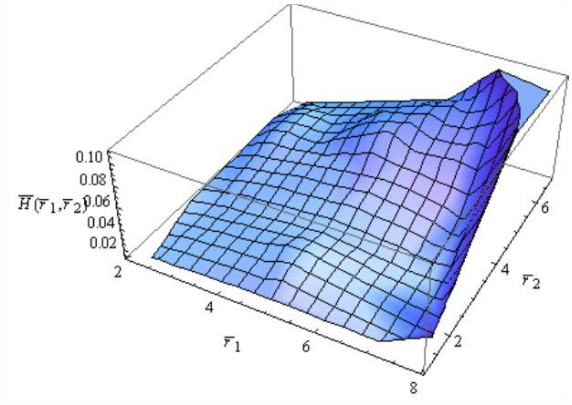

Figure 17. Truncated Joint hazard rate function that represents the probability of a sudden change in prices at values $\bar{r}_1$ and $\bar{r}_2$, provided they remain constant until that moment.

On the other hand, this type of graph is used practically to predict the chances of reaching certain price levels within short periods, especially in evaluating options or hedging instruments. This numerical experiment confirms that the proposed model can represent the constrained volatility environment and the probabilistic structure of price movements in multi-asset markets, supporting its use in financial market modeling, option pricing, and risk management. Furthermore, in practical implementation, the bounds $[a_i, b_i]$ and the time horizon $T = 1$ are assumed to be known to reflect realistic regulatory and empirical constraints of financial markets. These bounds correspond to the upper and lower daily price limits or to the empirically observed high-low ranges, as illustrated in Table 1. $T = 1$ assumption provides a normalized day of trading, and uniform time scale over assets. Calibration of the model within these known parameters with actual high-low observations greatly increases its practicability by aligning theoretical truncated probability framework to empirical market behavior. This calibration enhances the realism of the joint PMF, CDF, and hazard functions, improves the reliability of the model in forecasting volatility, and makes it more meaningful for real world applications to risk management, option pricing, and financial market analysis.

Based on the real financial data in this paper, the truncated and truncated Wiener multiple range model convincingly outperforms the unconstrained or closure only models. At the structure level, the model mimics the effect of price limit regimes by reconcentrating the mass of probability within the admissible region and condensing the tails near the limits, an empirical regularity documented in markets traded under price limit belts, as in [39]. Empirically, on the truncated ranges $\bar{r}_1 \in [2,8]$, $\bar{r}_2 \in [1,7]$ with $T = 1$, the truncated joint PMF exhibits inner peaks rather than edges, while the joint CDF increases smoothly as $(\bar{r}_1, \bar{r}_2)$ grows (see Figure 15). The truncated survival function and hazard rate are also consistent with the logic of restricted markets: For example, at (2.48,1.16), we obtain approximately

$$\bar{S}_{\bar{R}_i(T),\bar{R}_2(T)}(\bar{r}_1, \bar{r}_2; T) \approx 0.9952 \text{ and } \bar{H}_{\bar{R}_i(T),\bar{R}_2(T)}(\bar{r}_1, \bar{r}_2; T) \approx 0.016,$$

versus

$$\bar{S}_{\bar{R}_i(T),\bar{R}_2(T)}(\bar{r}_1, \bar{r}_2; T) \approx 0.267 \text{ and } \bar{H}_{\bar{R}_i(T),\bar{R}_2(T)}(\bar{r}_1, \bar{r}_2; T) \approx 0.080 \text{ at (6.42, 6.36),}$$

reflecting the risk buildup as the range widens near the boundary. These patterns are consistent with recent evidence showing that range dependent volatility models improve forecasting compared to close only specifications, and that range dependent GARCH formulas produce more robust estimates of volatility and tail risk in practice, as in [40]. They are also consistent with new findings on optimal nonparametric estimation of range volatility that establish the advantage of range information as in [41].

At the multivariate level, more recent research confirms the role of copulas (with dynamics) as a gold standard for reliability modeling and probabilistic forecasting of financial series, justifying the discrete binary treatment of the range employed here [42]. Finally, closed form equations of lumped survival/hazard equations provide directly interpretable joint exceedance probabilities on a discrete network, as in the expanding use of survival/hazard methods in financial econometrics [43]. Overall, through reasonably addressing regulatory constraints, discrete binary dependence, prediction power gains, and closed form lumped survival/hazard formulae, the model reflects a robust explanatory and predictive advantage over unconstrained or independence focused baselines, as shown in Figures 14–17.

5. Concluding remarks and future work

We present a multivariate, discrete type Wiener range distribution, aiming to build a rigorous mathematical framework for modeling the joint behavior of spreads (highs-lows) for several financial assets within range bound markets. The basic statistical properties of the distribution, such as the survival function, hazard function, truncated models, and stress-strength coefficient, are derived, demonstrating its suitability for realistic applications in volatility modeling and the valuation of risk sensitive financial instruments. A numerical application further supports the model's ability to capture realistic patterns in range constrained financial markets. This correspondence between the theoretical derivations and the numerical simulation results confirms the strong coherence of the proposed model with the actual behavior of constrained financial data, showing its empirical validity and robustness.

Although this framework assumes independence among marginal ranges for analytical tractability, in future research, we will extend the model to incorporate dependence structures between assets through copula based or correlated Wiener process formulations, enabling a more comprehensive representation of inter-asset dependence. In addition, we will address formal empirical validation of the Wiener process assumption and data driven estimation of truncation bounds through appropriate diagnostic tests and goodness of fit analyses based on real high-low range data. Further applications may include the pricing of range dependent derivatives and the design of algorithms for high frequency trading under stochastic constraints.

In addition to dependence modeling and empirical validation, an important direction for future research is to generalize the proposed framework beyond the Gaussian Wiener setting. Extending the discrete multivariate range distribution to non-Gaussian driving processes, such as Lévy-driven models or stochastic volatility formulations, would enable the model to capture heavy tailed behavior, jumps, and volatility clustering frequently observed in financial markets, while preserving the discrete and truncated structure of the proposed approach.

Author contributions

Sana Abdulkream Alharbi: Methodology, Visualization, Software, Writing-original draft; Mohamed Abd Allah El–Hadidy: Conceptualization, Methodology, Validation, Supervision, Writing-review and editing. All authors have read and approved the final version of the manuscript for publication.

Use of Generative-AI tools declaration

The authors declare they have not used Artificial Intelligence (AI) tools in the creation of this article.

Acknowledgements

This scientific paper is derived from a research grant funded by Taibah University, Madinah, Kingdom of Saudi Arabia - with grant number (447-15-1100).

Conflict of interest

The authors declare there is no conflict of interest.

References

1. M. Parkinson, The extreme value method for estimating the variance of the rate of return, *J. Bus.*, **53** (1980), 61–65.
2. M. Garman, M. Klass, On the estimation of security price volatilities from historical data, *J. Bus.*, **53** (1980), 67–78.
3. R. Cont, Empirical properties of asset returns: stylized facts and statistical issues, *Quant. Finance,* **1** (2001), 223–236. https://doi.org/10.1080/713665670
4. A. J. Patton, Modelling asymmetric exchange rate dependence, *Int. Econ. Rev.*, **47** (2006), 527–556. https://doi.org/10.1111/j.1468-2354.2006.00387.x
5. A. J. McNeil, R. Frey, P. Embrechts, *Quantitative Risk Management: Concepts, Techniques and Tools*, Princeton: Princeton University Press, 2015.
6. K. A. Kim, S. G. Rhee, Price limit performance: Evidence from the Tokyo stock exchange, *J. Finance*, **52** (1997), 885–901. https://doi.org/10.2307/2329504
7. W. Feller, The asymptotic distribution of the range of sums of independent random variables, *Ann. Math. Stat.*, **22** (1951), 427–432.
8. C. Withers, S. Nadarajah, The distribution and quantiles of the range of a Wiener process, *Appl. Math. Comput.*, **232** (2014), 766–770. https://doi.org/10.1016/j.amc.2014.01.147
9. A. Teamah, M. El-Hadidy, M. El-Ghoul, On bounded range distribution of a Wiener process, *Commun. Stat. Theory Methods*, **51** (2022), 919–942. https://doi.org/10.1080/03610926.2016.1267766
10. W. Kemp, Characterization of a discrete normal distribution, *J. Stat. Plan. Inference*, **63** (1997), 223–229. https://doi.org/10.1016/S0378-3758(97)00020-7
11. D. Roy, The discrete normal distribution, *Commun. Stat. Theory Methods*, **32** (2003), 1871–1883. https://doi.org/10.1081/STA-120023256
12. T. Nakagawa, S. Osaki, The discrete Weibull distribution, *IEEE Trans. Reliab.*, **24** (1975), 300–301.
13. K. Jayakumar, M. Girish Babu, Discrete Weibull geometric distribution and its properties, *Commun. Stat. Theory Methods*, **47** (2018), 1767–1783. https://doi.org/10.1080/03610926.2017.1327074
14. M. El-Hadidy, Discrete distribution for the stochastic range of a Wiener process and its properties, *Fluct. Noise Lett.*, **18** (2019), 1950024. https://doi.org/10.1142/S021947751950024X
15. M. El-Hadidy, A. Alfreedi, Internal truncated distributions: Applications to Wiener process range distribution when deleting a minimum stochastic volatility interval from its domain, *J. Taibah Univ. Sci.*, **13** (2019), 201–215. https://doi.org/10.1080/16583655.2018.1555020
16. C. Alexander, *Market Models: A Guide to Financial Data Analysis*, Hoboken: John Wiley & Sons, 2001.

17. R. Alraddadi, M. El-Hadidy, A multivariate model for the Wiener process range, with statistical properties under stochastic volatility, *AIMS Math.*, **10** (2025), 22023–22052. https://doi.org/10.3934/math.2025980
18. D. Pan, J. B. Liu, F. Huang, J. Cao, A. Alsaedi, A Wiener process model with truncated normal distribution for reliability analysis, *Appl. Math. Model.*, **50** (2017), 333–346. https://doi.org/10.1016/j.apm.2017.05.049
19. V. Sharma, Variance of some information measures for truncated random variables with applications, *PhD thesis, RGIPT, India*, 2024.
20. A. Aljadani, M. M. Mansour, H. M. Yousof, A novel model for finance and reliability applications, *Pak. J. Stat. Oper. Res.*, **20** (2024), 489–515. https://doi.org/10.18187/pjsor.v20i3.4439
21. S. J. Koopman, A. Lucas, M. Scharth, A. Opschoor, Dynamic discrete copula models for high-frequency stock price changes, *J. Appl. Econom.*, **33** (2018), 966–985. https://doi.org/10.1002/jae.2645
22. J. G. Skellam, The frequency distribution of the difference between two Poisson variates belonging to different populations, *J. R. Stat. Soc. Ser. A*, **109** (1946), 296. https://doi.org/10.1111/j.2397-2335.1946.tb04670.x
23. R. S. Tsay, *Analysis of Financial Time Series*, 3 Eds., Hoboken: John Wiley & Sons, 2010. https://doi.org/10.1002/9780470644560
24. A. Subrahmanyam, Circuit breakers and market volatility: A theoretical perspective, *J. Finance*, **49** (1994), 237–254. https://doi.org/10.2307/2329142
25. A. W. Marshall, I. Olkin, *Life Distributions*, Berlin: Springer, 2007.
26. M. Shaked, J. G. Shanthikumar, J. B. Valdez-Torres, Discrete hazard rate functions, *Comput. Oper. Res.*, **22** (1995), 391–402. https://doi.org/10.1016/0305-0548(94)00048-D
27. R. E. Barlow, F. Proschan, *Mathematical Theory of Reliability*, Philadelphia: SIAM, 1996.
28. M. Shaked, J. G. Shanthikumar, *Stochastic Orders*, Berlin: Springer, 2007. https://doi.org/10.1007/978-0-387-34675-5
29. D. Roy, R. P. Gupta, Characterizations and model selections through reliability measures in the discrete case, *Stat. Probab. Lett.*, **43** (1999), 197–206. https://doi.org/10.1016/S0167-7152(98)00260-0
30. F. J. Samaniego, *System Signatures and Their Applications in Engineering Reliability*, Berlin: Springer, 2007. https://doi.org/10.1007/978-0-387-71797-5
31. S. Kotz, N. Balakrishnan, N. L. Johnson, *Continuous Multivariate Distributions*, Hoboken: Wiley, 2000.
32. N. L. Johnson, S. Kotz, N. Balakrishnan, *Discrete Multivariate Distributions*, Hoboken: Wiley, 1994.
33. H. S. Wilf, *Generatingfunctionology*, Singapore: Academic Press, 2006. https://doi.org/10.1016/C2009-0-02369-1
34. F. W. J. Olver, *NIST Handbook of Mathematical Functions*, Cambridge: Cambridge University Press, 2010.
35. H. A. David, H. N. Nagaraja, *Order Statistics*, 3 Eds., Hoboken: Wiley, 2003.
36. B. C. Arnold, N. Balakrishnan, H. N. Nagaraja, *A First Course in Order Statistics*, Philadelphia: SIAM, 2008.
37. N. Balakrishnan, V. B. Nevzorov, *A Primer on Statistical Distributions*, Hoboken: Wiley, 2003.
38. S. Kotz, Y. Lumelskii, M. Pensky, *The Stress-Strength Model and and Its Generalizations*, Singapore: World Scientific, 2003. https://doi.org/10.1142/5015

39. O. Mnari, B. Faouel, Price limit bands, risk-return trade-off and asymmetric volatility, *Econ. Bus. Rev.*, **10** (2024), 142–162. https://doi.org/10.18559/ebr.2024.3.1604
40. M. Fałdziński, P. Fiszeder, P. Molnár, Improving volatility forecasts: Evidence from range-based models, *N. Am. J. Econ. Finance*, **69** (2024), 102019. https://doi.org/10.1016/j.najef.2023.102019
41. T. Bollerslev, J. Li, Q. Li, Optimal nonparametric range-based volatility estimation, *J. Econ.*, **238** (2024), 105548. https://doi.org/10.1016/j.jeconom.2023.105548
42. J. Zito, D. R. Kowal, A dynamic copula model for probabilistic forecasting of non-Gaussian multivariate time series, preprint paper, 2025. https://doi.org/10.48550/arXiv.2502.16874
43. MDPI Mathematics, *Application of survival analysis in economics, finance and insurance*, Special issue, 2024.